Establishment of porcine and human expanded potential stem cells

DOI:
10.1038/s41556-019-0333-2

Document Version
Accepted author manuscript

Citation for published version (APA):
Gao, X., Nowak-Imialek, M., Chen, X., Chen, D., Herrmann, D., Ruan, D., Chen, A. C. H., Eckersley-Maslin, M. A., Ahmad, S., Lee, Y. L., Kobayashi, T., Ryan, D., Zhong, J., Zhu, J., Wu, J., Lan, G., Petkov, S., Yang, J., Antunes, L., ... Liu, P. (2019). Establishment of porcine and human expanded potential stem cells. *Nature Cell Biology*, *21*(6), 687-699. https://doi.org/10.1038/s41556-019-0333-2

Published in:
Nature Cell Biology

Establishment of Porcine and Human Expanded Potential Stem Cells

Xuefei Gao[1,2*], Monika Nowak-Imialek[3*], Xi Chen[2*], Dongsheng Chen[4], Doris Herrmann[3], Degong Ruan[1,5], Andy Chun Hang Chen[6], Melanie A. Eckersley-Maslin[7], Ahmad Shakil[8], Yin Lau Lee[6], Toshihiro Kobayashi[9], David Ryan[2], Jixing Zhong[4], Jiacheng Zhu[4], Jian Wu[1], Guocheng Lan[10], Stoyan Petkov[3+], Jian Yang[2], Liliana Antunes[2], Lia S. Campos[2], Beiyuan Fu[2], Shengpeng Wang[4], Yong, Yu[2], Xiaomin Wang[5], Song-Guo Xue[11], Liangpeng Ge[12], Zuohua Liu[12], Yong Huang[12], Tao Nie[5], Peng Li[5], Donghai Wu[5], Duanqing Pei[5], Yi Zhang[13], Liming Lu[14], Fengtang Yang[2], Susan. J. Kimber[15], Wolf Reik[7], Xiangang Zou[10], Zhouchun Shang[4], Liangxue Lai[5], Azim Surani[9], Patrick P. L. Tam[16], Asif Ahmed[8], William Shu Biu Yeung[6], Sarah A. Teichmann[2], Heiner Niemann[3 §], Pentao Liu[1,2§]

1. The University of Hong Kong, Li Ka Shing Faculty of Medicine, School of Biomedical Sciences, Stem cell and regenerative medicine consortium, 5 Sassoon Road, Pokfulam, Hong Kong
2. The Wellcome Sanger Institute, Wellcome Genome Campus, Hinxton, Cambridge, CB10 1HH, UK
3. Institute of Farm Animal Genetics, Friedrich-Loeffler-Institut (FLI), Mariensee, 31535 Neustadt, Germany, and REBIRTH Centre of Excellence, Hannover Medical School, 30625 Hannover, Germany
4. BGI-Shenzhen, Shenzhen 518083 China, and China National GeneBank, BGI-Shenzhen, Shenzhen 518120, China.
5. Key Laboratory of Regenerative Biology, Guangzhou Institutes of Biomedicine and Health, Chinese Academy of Sciences, 510530 Guangzhou, China
6. Department of Obstetrics and Gynaecology, Li Ka Shing Faculty of Medicine, The University of Hong Kong, 21 Sassoon Road, Hong Kong
7. Epigenetics Programme, Babraham Institute, Babraham Research Campus, Cambridge, CB22 3AT, UK
8. Aston Medical School, Aston University, Birmingham B4 7ET, UK
9. Wellcome Trust and Cancer Research UK Gurdon Institute, University of Cambridge, Tennis Court Road, Cambridge CB2 1QN, UK
10. Cancer Research UK Cambridge Institute, University of Cambridge, Cambridge, CB2 0RE, UK
11. Center for Reproductive Medicine, Shanghai East Hospital, Tong Ji University School of Medicine. Shanghai 200120 China
12. Chongqing Academy of Animal Sciences, and Key Laboratory of Pig Industry Sciences, Department of Agriculture, Chongqing, 402460, China
13. Zhengzhou University first affiliated Hospital, Henan, China
14. Institute of Immunology, Shanghai Jiaotong University School of Medicine, Shanghai 200025, China

15. Faculty of Biology Medicine and Health, University of Manchester, Oxford Road, Manchester M13 9PT, U. K
16. Embryology Unit, Children's Medical Research Institute and School of Medical Sciences, Sydney Medical School, Faculty of Medicine and Health, The University of Sydney, Westmead, NSW 2145, Australia

[+]Present address: German Primate Center, Platform Degenerative Diseases Kellnerweg 4, 37077 Gottingen, Germany.

*Equal contribution

[§]Correspondence should be addressed to:
Pentao Liu, Ph.D. E-mail: pliu88@hku.hk or
Heiner Niemann, Ph.D. Present address: Hannover Medical School (MHH), TwinCore, 30625 Hannover. E-mail: niemann.heiner@mh-hannover.de

We recently derived mouse expanded potential stem cells (EPSCs) from individual blastomeres by inhibiting the critical molecular pathways that predispose their differentiation[1]. EPSCs had enriched molecular signatures of blastomeres and possessed the developmental potency for all embryonic and extraembryonic cell lineages. Here, we report the derivation of porcine EPSCs, which express key pluripotency genes, are genetically stable, permit genome editing, differentiate to derivatives of the three germ layers in chimeras, and produce primordial germ cell-like cells *in vitro*. Under similar conditions, human ESCs and iPSCs can be converted, or somatic cells directly reprogrammed, to EPSCs that display the molecular and functional attributes reminiscent of porcine EPSCs. Significantly, trophoblast stem cell-like cells can be generated from both human and porcine EPSCs. Our pathway-inhibition paradigm thus opens a new avenue for generating mammalian pluripotent stem cells, and EPSCs present an unique cellular platform for translational research in biotechnology and regenerative medicine.

Key words: pluripotent stem cells, totipotency, preimplantation embryos, porcine, chimeras, human, germ cells, iPS cell, trophoblast, placenta, single cell RNA sequencing, histone methylation, DNA methylation, developmental potential

Introduction

Mouse and human embryonic stem cells (ESCs) that derived from preimplantation embryos[2-4] self-renew in long term cultures and differentiate to all embryonic cell lineages *in vitro* and in mouse chimeras. The development of well-defined culture conditions such as 2i/LIF has substantially facilitated derivation and maintenance of mouse ESCs[5], and led to intensive efforts for deriving human ESCs akin to mouse ESCs[6,7]. It has however been challenging to translate the findings in studying mouse and human cells to establishing ESCs from other mammalian species. The domestic pig shares great genetic, anatomical and physiological similarities with humans, and is considered to be an excellent model for human diseases, cell therapies and even as donor for porcine xenografts. To this date, *bona fide* porcine ESCs have yet to be established.[8-15] The published lines usually do not meet with the stringent criteria for pluripotency and are frequently called "ES-like" cells.

We have recently demonstrated that by targeting key molecular pathways that drive lineage differentiation in the mouse preimplantation embryo, expanded potential stem cells (mEPSCs) displaying a broad propensity for extraembryonic and embryonic lineage differentiation were derived[1,16]. We hypothesized that a similar experimental paradigm of targeting key developmental pathways might be applied for establishing porcine stem cells from preimplantation embryos. However, little is known about the molecular and signalling mechanisms of porcine early preimplantation embryo development, we thus set out to perform a chemical screen of inhibitors that were used for isolating and maintaining mouse mEPSCs, mouse and human ESCs and to delineate the optimal condition for porcine cells. Our results demonstrate that porcine EPSCs could be established, and that significantly, similar culture conditions permit derivation of human EPSCs.

Results and Discussion

Identification of culture conditions for porcine pluripotent stem cells

While porcine iPSCs are available, their use for the screen is confounded by the leaky expression of the transgenic reprogramming factors after reprogramming or by low levels of expression of the endogenous pluripotency genes[17-20]. To overcome this challenge, we generated new porcine iPSCs by expressing Doxycycline (Dox)-inducible eight transcription factors, which substantially improved the efficiency of reprogramming wild-type and transgenic porcine fetal fibroblasts (PFFs), in which a *tdTomato* cassette had been inserted into the 3' UTR of the porcine *OCT4* (*POU5F1*) locus (POT PFFs)[21], to putative iPSC colonies (Fig. 1a-c). The iPSCs from POT PFFs were OCT4-tdTomato^{+}, (Fig. 1c), and expressed high levels of the endogenous pluripotency factors (Fig. 1d). iPSCs could be passaged as single cells for more than 20 passages in serum-containing medium (M15) plus Dox. Upon Dox removal, the iPSCs differentiated within 4-5 days, concomitant with rapid down-regulation of the exogenous reprogramming factors and endogenous pluripotency genes and with increased expression of both embryonic and extraembryonic cell lineage genes (Fig. 1e-h). These Dox-dependent iPSCs with robust endogenous pluripotency gene expression provided the material for the chemical screen.

In the screen, over 400 combinations of 20 small molecule inhibitors and cytokines were tested for their ability to maintain Dox-independent porcine iPSCs in the undifferentiated state (Fig. 1i; Supplementary Table 1). A departure was noted from previous reports that naïve mouse ESC medium 2i/LIF[5] was able to maintain putative porcine iPSCs[22-24]: Porcine iPSCs were rapidly lost with 1.0μM Mek1 inhibitor PD-0325901, irrespective of whether Dox was present or not (Extended Data Fig. 1a-g),

indicating that porcine pluripotent stem cells differ from mouse ESCs in the requirement of Mek-ERK signalling[5,25]. Inhibition of p38 and PKC was also non-conducive for porcine iPSCs (Extended Data Fig. 1f and 1h). Therefore mouse or human naïve ESC conditions[5-7] cannot be directly extrapolated to porcine cells. The inhibitors for Mek1/2, p38 and PKC were therefore excluded from the screen. Several conditions were identified that met the screen criteria (Extended Data Fig. 1g), including a minimal requisite condition (#517, porcine EPSC medium: pEPSCM) comprising inhibitors for GSK3 (CHIR99021), SRC (WH-4-023) and Tankyrases (XAV939) (the last two were inhibitors important for mouse EPSCs[1]) , and supplements: Vitamin C (Vc), ACTIVIN A and LIF (Fig. 1i. and Extended Data Fig. 1g and Supplementary Table 1). Under these conditions, the Dox-independent iPSCs ($pEPSC^{iPS}$) remained undifferentiated in 30 passages, expressed endogenous pluripotency factors at levels comparable to the porcine blastocyst and showed no leaky expression of the exogenous reprogramming factors (Fig. 1j, and Extended Data Fig. 1i-j).

We next repeated the reprogramming experiment by directly culturing the primary colonies in pEPSCM (Extended Data Fig. 2a), and generated 11 stable $pEPSC^{iPS}$ lines from 16 primary colonies (70% efficiency) with six of them having no detectable expression of any of the eight exogenous reprogramming factors but high levels of endogenous pluripotency genes (Extended Data Fig. 2b).

Establishment of porcine EPSCs from preimplantation embryos

The pEPSCM condition was subsequently employed to derive stem cell lines from porcine preimplantation embryos. A total of 26 lines ($pEPSCs^{Emb}$, 14 male and 12 female) were established from 76 early blastocysts (5.0 dpc), and 12 cell lines

(pEPSCs^{par}) from 252 parthenogenetic blastocysts (Fig. 2a, Supplementary Table 2 and Extended Data Fig. 2c). Similar to pEPSCs^{iPS}, pEPSCs^{Emb} had high nuclear/cytoplasmic ratios, and formed compact colonies with smooth colony edges (Fig. 2a, Extended Data Fig. 2d). pEPSCs^{Emb} were passaged every 3-4 days at 1:8 ratio as single cells, could be maintained for >40 passages on STO feeders without overt differentiation and were genetically stable (Extended Data Fig. 2e). Subcloning efficiency was about 10% at low cell density (2,000 cells per well in a 6-well plate), but routine passaging was performed at high cell density.

Pluripotency genes were expressed in pEPSCs^{Emb} and pEPSCs^{iPS} at levels comparable to the blastocysts (Fig. 2b and Extended Data Fig. 2b), but were drastically reduced or lost when pEPSCs were cultured in other porcine ESC media previously reported [9-15] (Extended Data Fig. 2f-g). pEPSCs showed extensive DNA demethylation at the *OCT4* and *NANOG* promoter regions (Fig. 2c) and had *OCT4* distal enhancer activity (Extended Data Fig. 2h). pEPSCs were amenable for Crispr/Cas9-mediated insertion of an *H2B-mCherry* expression cassette into the *ROSA26* locus (Extended Data Fig. 2i and 2j). *In vitro*, pEPSCs differentiated to tissues expressing genes representative of the three germ layers and, uniquely, trophoblast genes (Fig. 2d, Extended Data Fig. 2k). In immunocompromised mice, pEPSCs^{Emb} formed mature teratomas with derivatives of the three germ layers, and contained placental lactogen-1 (PL-1)-, KRT7- and SDC1-positive trophoblast-like cells (Fig. 2e-2f). Following incorporation of the pEPSCs into preimplantation embryos and after 48 hours of culture, pEPSCs (marked by H2B-mCherry) had colonized both the trophectoderm and inner cell mass of blastocysts (Extended Data Fig. 3a). Following transfer of the chimeric blastocysts to synchronized recipient sows, a total of 45 conceptuses were harvested from 3 litters at days 26-28 of gestation (Supplementary Table 3, Extended Data Fig. 3b). Flow

cytometry analysis of dissociated cells from embryonic and extraembryonic tissues of the chimeras detected mCherry$^+$ cells in 7 conceptuses (Extended Data Fig. 3c, Supplementary Table 4 and Table 5): mCherry$^+$ cells in both the placenta and embryonic tissues in 2 chimeras (#8 and #16); only in embryonic tissues in 3 chimeras (#4, #21 and #34); and exclusively in the placenta of 2 chimeras (#3 and #6). Genomic DNA PCR assays detected mCherry DNA only in those seven mCherry$^+$ chimeras, but not in any other conceptuses (Extended Data Fig. 3d, Supplementary Table 4 and 5). Despite the low contribution of the donor mCherry$^+$ cells, their descendants were found in multiple embryonic tissues and organs that were identified by tissue lineage markers (Fig. 2g and Extended Data Fig. 3e-f). Therefore, pEPSCs^{Emb} and pEPSCs^{iPS}, like mEPSCs, possess an expanded developmental potential for both the embryonic cell lineages and extra-embryonic trophoblast lineages.

Derivation of PGC-like cells (PGCLCs) from pEPSCs^{Emb}

We next asked if pEPSCs had the potential to produce PGCLCs *in vitro,* similar to mouse and human pluripotent stem cells[26-28]. In early-primitive streak (PS)-stage porcine embryos (E11.5–E12), the first cluster of porcine PGCs can be detected as SOX17$^+$ cells in the posterior end of the nascent primitive streak, and these cells later co-express OCT4, NANOG, BLIMP1 and TFAP2C[28]. *NANOS3* is an evolutionarily conserved PGC-specific factor[29,30] and human *NANOS3* reporter ESCs have been used for studying the derivation of PGCLCs[27,28]. We generated and used a *NANOS3-H2B-mCherry* pEPSC^{Emb} reporter line to facilitate identification of putative PGCLCs (Extended Data Fig. 4a). After expressing the *SOX17* transgene transiently for 12 hours, the reporter cells were allowed to form embryoid bodies (EBs) (Extended Data

Fig. 4b), where cell clusters co-expressing *NANOS3* (mCherry^{+}) and tissue-nonspecific alkaline phosphatase (TNAP, a PGC marker) were detected within 3-4 days (Fig. 3a).

The derivation of putative porcine PGCLCs was BMP2/4 dependent (Fig. 3a). Interestingly, different from the reported derivation of human PGCLCs[28], expressing *NANOG*, *BLIMP1* or *TFAP2C* transgenes, either individually or in combination, had no effect on the preponderance of *NANOS3*$^{+}$ cells (Extended Data Fig. 4c), whereas co-expression of *SOX17* with *BLIMP1* appeared to increase *NANOS3*$^{+}$ cells (Extended Data Fig. 4c and 4d).

The putative PGCLCs within the EBs expressed PGC-specific genes (Fig. 3b-c, and Extended Data Fig. 4e). Specific RNA-seq analysis of *NANOS3*$^{+}$ cells revealed expression of early PGC genes[27] (*OCT4*, *NANOG*, *LIN28A*, *TFAP2C*, *CD38*, *DND1*, *NANOS3*, *ITGB3*, *SOX15* and *KIT*), and reduced *SOX2* expression (Fig. 3d-e). Similar to PGCLC derivation from human ESCs[27], *DNMT3B* was down-regulated in porcine mCherry^{+}/*NANOS3*$^{+}$ cells whereas *TET1/2* were up-regulated, relative to the parental pEPSCs^{Emb} (Fig. 3e-f).

Establishment of human EPSCs under conditions similar to porcine EPSCs

The finding that inhibition of SRC and Tankyrases is sufficient to convert mouse ESCs to mEPSCs[1] and that the same two inhibitors are required for the derivation of pEPSCs raises the possibility that similar *in vitro* culture conditions may be developed for additional mammalian species. To explore this possibility, we cultured four established human ES cell (hESC) lines (H1, H9, Man1/M1, and Man10/M10 cells)[4,31,32] in pEPSCM and passaged them three times. The cells displayed diverse morphologies and heterogeneous expression of OCT4 (Extended Data Fig. 5a).

Removing ACTIVIN A (20.0 ng/ml) from pEPSCM led to considerably fewer cell colonies formed from H1 (<1.0%) and M1 (5.0%) ESCs, while none from H9 or M10 (Extended Data Fig. 5a), which reflects the inherent between-line heterogeneity of human ESCs[33,34]. With further refinement of the culture conditions (for example, replacing WH-4-023 with another SRC inhibitor A419259 in hEPSCM, see Methods), morphologically homogenous and stable cell lines were established from single-cell sub-cloned H1 (H1-EPSCs) and M1 cells (M1-EPSCs) (Fig. 4a). Karyotype analysis of H1 and M1 cells grown in hEPSCM on STO feeders revealed genetic stability (at passage 25 post conversion from the parental hESCs, Extended Data Fig. 5b). When human primary iPSC colonies reprogrammed from fibroblasts were directly cultured in hEPSCM, around 70% of the picked colonies could be established as stable iPSC lines (iPSC-EPSCs) (Extended Data Fig. 5c), which expressed pluripotency markers with no obvious leakiness of the exogenous reprogramming factors in about half of the lines (Fig. 4b and Extended Data Fig. 5d). The H1-EPSCs proliferated more robustly than the H1 ESCs cultured in standard FGF-containing medium (H1-ESC, primed) or under naïve 5i/L/A conditions (H1-naïve ESC)[7] (Extended Data Fig. 5e), and were tolerant of single cell passaging with about 10% single cell sub-cloning efficiency in the transient presence of ROCKi. Cell survival at passaging was substantially improved in the presence of 5.0ng/ml ACTIVIN A or by splitting the cells at higher density. Human EPSCs expressed pluripotency genes at higher levels than the H1-ESCs (Fig. 4b) and minimal levels of lineage markers (Extended Data Fig. 5f). Expression of core pluripotency factors and surface markers in human EPSCs was confirmed by immunostaining (Extended Data Fig. 5g). H1-EPSCs differentiated to derivatives of the three germ layers *in vitro* and *in vivo* (Extended Data Fig. 5h-i). Moreover, H1-EPSCs were successfully differentiated to PGCLCs

using *in vitro* conditions developed for germ cell competent hESCs or iPSCs[27,28] (Fig. 4c and Extended Data Fig. 5j).

Our results demonstrate that porcine and human EPSCs could be derived and maintained using the similar set of small molecule inhibitors. Global gene expression profiling revealed that pEPSCs and hEPSCs were clustered together, and were distinct from PFFs or other human pluripotent stem cells[1,35,36] (Fig. 4d-e). Both porcine and human EPSCs expressed high levels of key pluripotency genes, low levels of somatic cell lineage genes, *PAX6*, *T*, *GATA4* and *SOX7*, or placenta-related genes (*PGF*, *TFAP2C*, *EGFR*, *SDC1* and *ITGA5*) (Extended Data Fig. 6a-d). Consistent with the high levels of global DNA methylation of pEPSCs and hEPSCs (Extended Data Fig. 6e), DNA methyltransferase genes *DNMT1* and *DNMT3A* and *DNMT3B* were highly expressed, whereas *TET1*, *TET2* and *TET3* were expressed at lower levels (Extended Data Fig. 6f-g). Among the highly expressed 76 genes (>8-fold increase) in H1-EPSC in comparison to H1-ESCs, 17 genes encode histone variants with 15 belonging to the histone cluster 1 (Fig. 4f and Supplementary Table 6). nterestingly, these histone genes were expressed at low levels in 5i and primed human ESCs but were highly expressed in human 8-cell and morula stage embryos (Fig. 4g). The significantly higher expression of these histone genes was confirmed in additional hEPSC lines (Fig. 4h). The biological significance of this observation remains to be investigated.

Single cell RNA-seq (scRNAseq) reveals substantially homogenous EPSC cultures

EPSCs expressed uniform levels of the core pluripotency factors (Fig. 5a) and were generally homogenous cells in culture in the context of single-cell transcriptome (Fig. 5b). Mouse EPSCs had enriched transcriptomic features of 4-cell to 8-cell

blastomeres[1]. scRNAseq analysis suggested that hEPSCs were transcriptionally, as well as the histone gene expression profiles, more similar to human 8-cell to morula stage embryos[37,38] than other stages of preimplantation embryos (Fig. 5c, and Extended Data Figure 6h; Fig. 4g-hand Extended Data Fig. 6i). Interestingly, single-cell transcriptome also revealed low expression of naïve pluripotency factors such as *KLF2* in EPSCs (Fig. 5a and Extended Data Fig. 6a-b), which is also not highly expressed in human early preimplantation embryos[39]. Although *KLF2*, *TET1*, *TET2* and *TET3* were weakly expressed in both pEPSCs and hEPSCs (Extended Data Fig. 6a-b and 6f-g), their promoter regions were characterized by active H3K4m3 histone marks (Fig. 5d-e). In contrast to pluripotency genes, in both porcine and human EPSCs, the cell lineage gene loci (e.g. *CDX2*, *GATA2*, *GATA4*, *SOX7* and *PDX1*) had high H3K27me3 and low H3K4me3 marks, respectively (Fig. 5e).

Human and porcine EPSCs have similar signalling requirements

To identify signalling requirements in EPSCs, we removed individual components from the culture medium. Removal of the SRC inhibitor WH-4-023 or A419259 reduced expression of pluripotency factors in both EPSCs (Fig. 6a-d). Notably, in hEPSCs, using the SRC inhibitor WH-4-023 instead of A419259 led to lower pluripotency gene expression (Fig. 6b). Similar to mEPSCs, XAV939 enhanced AXIN1 protein content (Fig. 6e), and reduced canonical WNT activities in both EPSCs (Fig. 6f). Withdrawal of XAV939 caused collapse of pluripotency and differentiation of these EPSCs (Fig. 6a-b, 6d, and 6g-k). SMAD2/3 were phosphorylated in EPSCs (Fig. 6e). Either removing ACTIVIN A from pEPSCM or adding the TGFβ inhibitor SB431542 resulted in massive cell loss and down-regulation of pluripotency factors in pEPSCs (Fig. 6a, 6g, 6h and 6j). hEPSCs did not require exogenous TGFB in culture but inhibiting TGFβ induced rapid cell

differentiation with preferential expression of trophoblast genes *CDX2*, *ELF5* and *GATA2* (Fig. 6b, 6i and 6k). At a relatively low concentration of ACTIVIN A (5.0ng/ml), hEPSCs showed a stronger propensity for embryonic mesendoderm lineage differentiation (Fig. 6l) and generated more NANOS3-tdTomato$^+$ PGCLCs (Fig. 6m-n). Removing CHIR99021 and Vitamin C from EPSCM did not affect pluripotency gene expression but reduced the number of colonies formed from single cells (Fig. 6a-b and 6h-i), whereas a high CHIR99021 concentration (3.0μM) induced differentiation of both EPSCs (Fig. 6a, 6h and 6j), similar to that in human or rat naïve cells[6,40]. JNK and BRAF inhibition might improve culture efficiency but was not essential (Fig. 6h-i). Mouse naïve ESCs is cultured 1.0μM Mek1/2 inhibitor PD0325901 (Ref. 5). We noticed that even 0.1 μM PD0325901 decreased pEPSC survival as measured by colony formation in serial passaging (Fig. 6h).

hEPSCs have potent potential to trophoblasts

We further investigated differentiation of hEPSCs to trophoblasts by generating the *CDX2-Venus* reporter line (Extended Data Fig. 7a). Inhibiting TGFβ by SB431542 resulted in ~70% of the reporter cells being CDX2-Venus$^+$ (Fig. 7a), whereas essentially no *CDX2-Venus*$^+$ cells were detected if the reporter cells were previously cultured in FGF or under the 5i naïve ESC conditions. Consistently, trophoblast gene levels were rapidly increased in differentiated H1-EPSCs and iPSC-EPSCs but not in H1-ESCs or H1-5i naïve cells (Fig. 7b). Addition of BMP4, which promotes differentiation of human ESCs to putative trophoblasts[41], induced a much higher level of expression of trophoblast genes in EPSCs than in H1-ESCs or H1-5i naïve ESCs (Extended Data Fig. 7b). Inhibiting FGF and TGFβ signalling while in parallel activating BMP4 was reported to effectively induce trophoblast differentiation of

human ESCs[42,43]. Under these conditions, expression of trophoblast genes, especially the late trophoblast genes *GCM1*, *CGA* and *CGB*, was much higher in H1-EPSCs than in H1-ESCs, whereas naïve 5i hESCs displayed no sign of trophoblast differentiation (Extended Data Fig. 7c). Global gene expression analysis demonstrated that under TGFβ signalling inhibition H1-EPSCs and iPSC-EPSCs followed a differentiation trajectory distinct from that of H1-ESCs (Fig. 7c), and that in cells differentiated from EPSCs, but not from H1-ESCs, genes associated with trophoblast development or function were highly expressed including: (1) *BMP4* (Day 2-4); (2) *Syncytin-1* (*ERVW-1*) and *Syncytin-2* (*ERVFRD-1*) that promote cytotrophoblast fusion into syncytiotrophoblast; (3) *p57* (encoded by CDKN1C) [44,45]; (4) *CD274* (encoding PD-L1 or B7-H1); and (5) *EGFR*[46] (Fig. 7d).

We next performed Pearson correlation coefficient analysis of the transcriptome of cells differentiated under TGFβ inhibition with published reference data of primary human trophoblasts (PHTs) and human placenta tissues[43], which again revealed the similarity between cells differentiated from hEPSCs and PHTs and the placenta (Extended Data Fig. 7d). The differentiated cells from H1-EPSCs expressed human trophoblast specific miRNAs (C19MC miRNAs: hsa-miR-525-3p, hsa-miR-526b-3p, hsa-miR-517-5p, and hsa-miR-517b-3p)[47] (Extended Data Fig. 7e-f), displayed DNA demethylation at the *ELF5* locus[48,49] (Fig. 7e), and produced abundant amounts of placental hormones (Fig. 7f-g).

One key mechanism for derivation and maintenance of EPSCs of mouse, porcine and human is blocking poly(ADP-ribosyl)ation activities of PARP family members TNKS1/2 using small molecule inhibitors such as XAV939[50,51]. In human cells, poly(ADP-ribose) in proteins is removed by poly(ADP-ribose) glycohydrolase

(PARG) and ADP-ribosylhydrolase 3 (ARH3)[52]. Genetic inactivation of *Parp1/2* and *TNKS1/2* in the mouse caused trophoblast phenotypes[53], whereas inactivating *Parg* led to loss of functional trophectoderm and trophoblast stem cell (TSCs)[54]. In hEPSCs, *PARG*-deficiency did not appear to cause noticeable changes in EPSCs but adversely affected trophoblast differentiation (Extended Data Fig. 7g-j), which may indicate an evolutionally conserved mechanism for EPSCs and trophoblast development between mouse and human.

Derivation of TSC-like cells from human and porcine EPSCs

When hEPSCs (ESC-converted-EPSCs and iPSC-EPSCs) were cultured in human TSC conditions[46] with low cell density (2,000 cells/3.5cm dish), colonies with TSC morphology formed after 7-9 days (Fig. 8a). These colonies were picked and expanded into stable cell lines under TSC conditions with up to 30% efficiency in line establishment. These hEPSC-derived TSC-like cells were referred in this study as hTSCs. In contrast, no lines were established from human H1 or M1 ESCs under the hTSC condition, whether they were originally cultured under primed or naïve ESCs conditions. The hTSCs expressed trophoblast transcription regulators: GATA3 and TFAP2C but had down-regulated pluripotency genes (Fig. 8b-c), and showed enriched transcriptomic features of day-4 differentiated human EPSCs under TGFβ inhibition (Fig. 8d). Following the published protocols[46], we were able to differentiate hTSCs to multi-nucleated syncytiotrophoblasts (ST) and HLA-G$^+$ extravillous trophoblasts (EVT) (Fig. 8e-i). Once injected into immunocompromised mice, hTSCs formed lesions with cells positively stained for SDC1 and KRT7 (Fig. 8j-k). Additionally, high levels of hCG were detected in blood of the mice with hTSC-lesions but not in control mice injected with vehicle only (Fig.8l). Although neither EPSCs expressed high levels of placenta development-related genes (Extended Data

Fig. 6c-d), both displayed enriched H3K4me3 at these loci (Extended Data Fig. 8a), clearly underpinning EPSCs' trophoblast potency. Under hTSC conditions, stable TSC-like lines could also be derived from pEPSCs^{Emb} (pTSCs). Extended Data Fig. 8b). pTSCs were similar to hTSCs in gene expression profiles and the propensity of lesion formation in immunocompromised mice (Extended Data Fig. 8c-f). When introduced into porcine preimplantation embryos, descendants of pTSCs were found in the trophectoderm and expressed GATA3 and CDX2 (Extended Data Fig. 8g). Our results therefore provide compelling evidence that human and porcine EPSCs possessed expanded potential that encompasses the trophoblast lineage.

In conclusion, EPSCs of mouse, pig and human can now be established under similar *in vitro* culture conditions. These stem cells share common molecular features and possess expanded potency for both embryonic and extraembryonic cell lineages that are generally not seen in the conventional embryo-derived or induced pluripotent stem cells. EPSCs therefore represents a unique state of cellular potency. The successful generation of EPSCs produces new tools for investigation of embryonic development and opens new avenues for translational research in biotechnology, agriculture, and genomics and regenerative medicine.

References

1 Yang, J. *et al.* Establishment of mouse expanded potential stem cells. *Nature* **550**, 393-397, doi:10.1038/nature24052 (2017).

2 Evans, M. J. & Kaufman, M. H. Establishment in culture of pluripotential cells from mouse embryos. *Nature* **292**, 154-156 (1981).

3 Martin, G. R. Isolation of a pluripotent cell line from early mouse embryos cultured in medium conditioned by teratocarcinoma stem cells. *Proceedings of the National Academy of Sciences of the United States of America* **78**, 7634-7638 (1981).

4 Thomson, J. A. *et al.* Embryonic stem cell lines derived from human blastocysts. *Science* **282**, 1145-1147 (1998).

5 Ying, Q. L. *et al.* The ground state of embryonic stem cell self-renewal. *Nature* **453**, 519-523, doi:10.1038/nature06968 (2008).
6 Takashima, Y. *et al.* Resetting Transcription Factor Control Circuitry toward Ground-State Pluripotency in Human. *Cell* **158**, 1254-1269, doi:10.1016/j.cell.2014.08.029 (2014).
7 Theunissen, T. W. *et al.* Systematic identification of culture conditions for induction and maintenance of naive human pluripotency. *Cell stem cell* **15**, 471-487, doi:10.1016/j.stem.2014.07.002 (2014).
8 Ezashi, T., Yuan, Y. & Roberts, R. M. Pluripotent Stem Cells from Domesticated Mammals. *Annu Rev Anim Biosci* **4**, 223-253, doi:10.1146/annurev-animal-021815-111202 (2016).
9 Brevini, T. A. *et al.* Culture conditions and signalling networks promoting the establishment of cell lines from parthenogenetic and biparental pig embryos. *Stem Cell Rev* **6**, 484-495, doi:10.1007/s12015-010-9153-2 (2010).
10 Vassiliev, I. *et al.* In vitro and in vivo characterization of putative porcine embryonic stem cells. *Cell Reprogram* **12**, 223-230, doi:10.1089/cell.2009.0053 (2010).
11 Haraguchi, S., Kikuchi, K., Nakai, M. & Tokunaga, T. Establishment of self-renewing porcine embryonic stem cell-like cells by signal inhibition. *J Reprod Dev* **58**, 707-716 (2012).
12 Park, J. K. *et al.* Primed pluripotent cell lines derived from various embryonic origins and somatic cells in pig. *PLoS One* **8**, e52481, doi:10.1371/journal.pone.0052481 (2013).
13 Hou, D. R. *et al.* Derivation of Porcine Embryonic Stem-Like Cells from In Vitro-Produced Blastocyst-Stage Embryos. *Sci Rep* **6**, 25838, doi:10.1038/srep25838 (2016).
14 Xue, B. *et al.* Porcine Pluripotent Stem Cells Derived from IVF Embryos Contribute to Chimeric Development In Vivo. *PLoS One* **11**, e0151737, doi:10.1371/journal.pone.0151737 (2016).
15 Ma, Y., Yu, T., Cai, Y. & Wang, H. Preserving self-renewal of porcine pluripotent stem cells in serum-free 3i culture condition and independent of LIF and b-FGF cytokines. *Cell Death Discov* **4**, 21, doi:10.1038/s41420-017-0015-4 (2018).
16 Yang, J., Ryan, D. J., Lan, G., Zou, X. & Liu, P. In vitro establishment of expanded-potential stem cells from mouse pre-implantation embryos or embryonic stem cells. *Nat Protoc*, doi:10.1038/s41596-018-0096-4 (2019).
17 Esteban, M. A. *et al.* Generation of induced pluripotent stem cell lines from Tibetan miniature pig. *J Biol Chem* **284**, 17634-17640, doi:10.1074/jbc.M109.008938 (2009).
18 Ezashi, T. *et al.* Derivation of induced pluripotent stem cells from pig somatic cells. *Proc Natl Acad Sci U S A* **106**, 10993-10998, doi:10.1073/pnas.0905284106 (2009).
19 West, F. D. *et al.* Porcine induced pluripotent stem cells produce chimeric offspring. *Stem Cells Dev* **19**, 1211-1220, doi:10.1089/scd.2009.0458 (2010).
20 Petkov, S., Glage, S., Nowak-Imialek, M. & Niemann, H. Long-Term Culture of Porcine Induced Pluripotent Stem-Like Cells Under Feeder-Free Conditions in the Presence of Histone Deacetylase Inhibitors. *Stem Cells Dev* **25**, 386-394, doi:10.1089/scd.2015.0317 (2016).
21 Lai, S. *et al.* Generation of Knock-In Pigs Carrying Oct4-tdTomato Reporter through CRISPR/Cas9-Mediated Genome Engineering. *PLoS One* **11**, e0146562, doi:10.1371/journal.pone.0146562 (2016).
22 Zhang, W. *et al.* Pluripotent and Metabolic Features of Two Types of Porcine iPSCs Derived from Defined Mouse and Human ES Cell Culture Conditions. *PLoS One* **10**, e0124562, doi:10.1371/journal.pone.0124562 (2015).

23 Telugu, B. P., Ezashi, T. & Roberts, R. M. Porcine induced pluripotent stem cells analogous to naive and primed embryonic stem cells of the mouse. *Int J Dev Biol* **54**, 1703-1711, doi:10.1387/ijdb.103200bt (2010).
24 Du, X. *et al.* Barriers for Deriving Transgene-Free Pig iPS Cells with Episomal Vectors. *Stem Cells* **33**, 3228-3238, doi:10.1002/stem.2089 (2015).
25 Chen, H. *et al.* Erk signaling is indispensable for genomic stability and self-renewal of mouse embryonic stem cells. *Proc Natl Acad Sci U S A* **112**, E5936-E5943 (2015).
26 Hayashi, K., Ohta, H., Kurimoto, K., Aramaki, S. & Saitou, M. Reconstitution of the mouse germ cell specification pathway in culture by pluripotent stem cells. *Cell* **146**, 519-532, doi:10.1016/j.cell.2011.06.052 (2011).
27 Irie, N. *et al.* SOX17 is a critical specifier of human primordial germ cell fate. *Cell* **160**, 253-268, doi:10.1016/j.cell.2014.12.013 (2015).
28 Kobayashi, T. *et al.* Principles of early human development and germ cell program from conserved model systems. *Nature* **546**, 416-420, doi:10.1038/nature22812 (2017).
29 Julaton, V. T. & Reijo Pera, R. A. NANOS3 function in human germ cell development. *Hum Mol Genet* **20**, 2238-2250, doi:10.1093/hmg/ddr114 (2011).
30 Gkountela, S. *et al.* The ontogeny of cKIT+ human primordial germ cells proves to be a resource for human germ line reprogramming, imprint erasure and in vitro differentiation. *Nat Cell Biol* **15**, 113-122, doi:10.1038/ncb2638 (2013).
31 Camarasa, M. V. *et al.* Derivation of Man-1 and Man-2 research grade human embryonic stem cell lines. *In Vitro Cell Dev Biol Anim* **46**, 386-394, doi:10.1007/s11626-010-9291-5 (2010).
32 Ye, J. *et al.* High quality clinical grade human embryonic stem cell lines derived from fresh discarded embryos. *Stem Cell Res Ther* **8**, 128, doi:10.1186/s13287-017-0561-y (2017).
33 International Stem Cell, I. *et al.* Characterization of human embryonic stem cell lines by the International Stem Cell Initiative. *Nat Biotechnol* **25**, 803-816, doi:10.1038/nbt1318 (2007).
34 Koyanagi-Aoi, M. *et al.* Differentiation-defective phenotypes revealed by large-scale analyses of human pluripotent stem cells. *Proc Natl Acad Sci U S A* **110**, 20569-20574, doi:10.1073/pnas.1319061110 (2013).
35 Theunissen, T. W. *et al.* Molecular Criteria for Defining the Naive Human Pluripotent State. *Cell Stem Cell* **19**, 502-515, doi:10.1016/j.stem.2016.06.011 (2016).
36 Yang, Y. *et al.* Derivation of Pluripotent Stem Cells with In Vivo Embryonic and Extraembryonic Potency. *Cell* **169**, 243-257 e225, doi:10.1016/j.cell.2017.02.005 (2017).
37 Yan, L. *et al.* Single-cell RNA-Seq profiling of human preimplantation embryos and embryonic stem cells. *Nat Struct Mol Biol* **20**, 1131-1139, doi:10.1038/nsmb.2660 (2013).
38 Dang, Y. *et al.* Tracing the expression of circular RNAs in human pre-implantation embryos. *Genome Biol* **17**, 130, doi:10.1186/s13059-016-0991-3 (2016).
39 Blakeley, P. *et al.* Defining the three cell lineages of the human blastocyst by single-cell RNA-seq. *Development* **142**, 3613, doi:10.1242/dev.131235 (2015).
40 Chen, Y., Blair, K. & Smith, A. Robust Self-Renewal of Rat Embryonic Stem Cells Requires Fine-Tuning of Glycogen Synthase Kinase-3 Inhibition. *Stem cell reports* **1**, 209-217, doi:10.1016/j.stemcr.2013.07.003 (2013).
41 Xu, R. H. *et al.* BMP4 initiates human embryonic stem cell differentiation to trophoblast. *Nat Biotechnol* **20**, 1261-1264, doi:10.1038/nbt761 (2002).

42 Amita, M. *et al.* Complete and unidirectional conversion of human embryonic stem cells to trophoblast by BMP4. *Proc Natl Acad Sci U S A* **110**, E1212-1221, doi:10.1073/pnas.1303094110 (2013).
43 Yabe, S. *et al.* Comparison of syncytiotrophoblast generated from human embryonic stem cells and from term placentas. *Proc Natl Acad Sci U S A* **113**, E2598-2607, doi:10.1073/pnas.1601630113 (2016).
44 Chilosi, M. *et al.* Differential expression of p57kip2, a maternally imprinted cdk inhibitor, in normal human placenta and gestational trophoblastic disease. *Lab Invest* **78**, 269-276 (1998).
45 Zhang, P., Wong, C., DePinho, R. A., Harper, J. W. & Elledge, S. J. Cooperation between the Cdk inhibitors p27(KIP1) and p57(KIP2) in the control of tissue growth and development. *Genes Dev* **12**, 3162-3167 (1998).
46 Okae, H. *et al.* Derivation of Human Trophoblast Stem Cells. *Cell Stem Cell* **22**, 50-63 e56, doi:10.1016/j.stem.2017.11.004 (2018).
47 Lee, C. Q. *et al.* What Is Trophoblast? A Combination of Criteria Define Human First-Trimester Trophoblast. *Stem Cell Reports* **6**, 257-272, doi:10.1016/j.stemcr.2016.01.006 (2016).
48 Hemberger, M., Udayashankar, R., Tesar, P., Moore, H. & Burton, G. J. ELF5-enforced transcriptional networks define an epigenetically regulated trophoblast stem cell compartment in the human placenta. *Hum Mol Genet* **19**, 2456-2467, doi:10.1093/hmg/ddq128 (2010).
49 Ng, R. K. *et al.* Epigenetic restriction of embryonic cell lineage fate by methylation of Elf5. *Nat Cell Biol* **10**, 1280-1290, doi:10.1038/ncb1786 (2008).
50 Huang, S. M. *et al.* Tankyrase inhibition stabilizes axin and antagonizes Wnt signalling. *Nature* **461**, 614-620, doi:10.1038/nature08356 (2009).
51 Thorsell, A. G. *et al.* Structural Basis for Potency and Promiscuity in Poly(ADP-ribose) Polymerase (PARP) and Tankyrase Inhibitors. *J Med Chem* **60**, 1262-1271, doi:10.1021/acs.jmedchem.6b00990 (2017).
52 Hassa, P. O. & Hottiger, M. O. The diverse biological roles of mammalian PARPS, a small but powerful family of poly-ADP-ribose polymerases. *Front Biosci* **13**, 3046-3082 (2008).
53 Hemberger, M. *et al.* Parp1-deficiency induces differentiation of ES cells into trophoblast derivatives. *Developmental biology* **257**, 371-381 (2003).
54 Koh, D. W. *et al.* Failure to degrade poly(ADP-ribose) causes increased sensitivity to cytotoxicity and early embryonic lethality. *Proc Natl Acad Sci U S A* **101**, 17699-17704, doi:10.1073/pnas.0406182101 (2004).

Acknowledgements

We thank colleagues of the Wellcome Trust Sanger Institute core facilities for generous support (James Bussell, Yvette Hooks, N. Smerdon, B. L. Ng and J. Graham), and Professor Ashley Moffett for critical comments. We acknowledge the following funding and supports: The Wellcome Trust (grant numbers 098051 and 206194) to the Sanger Institute, and The University of Hong Kong internal funding (P. Liu); Wellcome Trust Clinical PhD Fellowship for Academic Clinicians (D.J.R.);

PhD fellowship (Portuguese Foundation for Science and Technology, FCT (SFRH/BD/84964/2012) (L.A.), Marie Sklodowska-Curie Individual Fellowship (M.A.E.-M.); BBSRC (grant BB/K010867/1), Wellcome Trust (grant 095645/Z/11/Z), EU EpiGeneSys, and BLUEPRINT (W.R.); Chongqing Agriculture Development Grant (17407 for L.P.G., Z.H.L., and Y.H.; REBIRTH project No. 9.1, Hannover Medical School (MHH) (for H.N.); Shuguang Planning of Shanghai Municipal Education Commission (16SG14) and The National Key Research and Development Program (2017YFA0104500) (L. Lu); China Postdoctoral Science Foundation (grant 2017M622795) (D.C.); Shenzhen Municipal Government of China (DRC-SZ [2016] 884) (Z.S.); NHMRC of Australia (Senior Principal Research Fellowship, Grant 1110751 (P.P.L.T.); GRF of Hong Kong (17119117 and 17107915) and National Natural Science Foundation (81671579 for L. Lu; 31471398 for W.S.B.Y.; and U1804281 for Y. Zhang). The authors thank Dr. Bjoern Petersen for performing the surgical embryo transfers and staff of the experimental pig facility in Friedrich-Loeffler-Institut Mariensee for competent and enduring assistance.

Author contributions

X.G. developed the culture conditions for pEPSCs and hEPSCs and performed most of the experiments; MN performed the pig experiments and wrote the paper; DH was critically involved in all porcine experiments; SP provided some pig reprogramming factor genes; XC performed most of the informatics analysis and ST supported XC; DC, SW, JZho, JZhu and ZS analyzed RNAseq data of hEPSCs/ESCs to trophoblasts; ACHC, YLL and WSBY performed teratoma and TSC lesion at the HKU; and MEM and WR performed EPSC DNA methylation analysis; TK and AS helped XG on PGCLC analysis; AH and AA measured hormones in cells differentiated from

hEPSCs; LC analysed teratoma sections; YF and FB karyotyped cells; DR, XW, LG, ZL, YH, TN, DW, DP, LLai, GL, DRyan, JY, LA, YY, SGX, YZ, LLu, ZX were involved in refining the culture conditions or intellectual inputs; SJK provided human M1 and M10 ESCs; PPLT provided intellectual inputs and edited the manuscript; HN conceptualized pig experiments, wrote paper, secured funding for the pig part of the experiments; PL conceived the pEPSC culture screen concept, supervised the research and wrote paper.

Figure legends

Figure 1. **Identification of culture conditions for porcine EPSCs**. **a**. Doxycycline (Dox)-inducible expression of Yamanaka factors *OCT4*, *MYC, SOX2* and *KLF4*, together with *LIN28*, *NANOG*, *LRH1* and *RARG* in porcine PFFs. Stable genomic integration of cDNAs in PFFs was achieved by piggyBac transposition. pOMSK: Porcine *OCT4*, *MYC, SOX2* and *KLF4; p*N+hLIN: porcine *NANOG* and human *LIN28*; hRL: human *RARG* and *LRH1*. The reprogrammed colonies were single-cell passaged in the presence of Dox in M15 (15% fetal calf serum). **b**. Co-expression of *LIN28*, *NANOG*, *LRH1* and *RARG* substantially increased the number of reprogrammed colonies from 250,000 PFFs (n = 4 independent experiments). **c**. Reprogramming of the porcine *OCT4-tdTomato* knock-in reporter (POT) TAIHU and wide type (WT) German Landrace PFFs to iPSCs. **d**. The iPSCs lines expressed key pluripotency genes in RT-qPCR analysis. The iPSC lines $^{\#}$1 and $^{\#}$2, and iPSC $^{\#}$3 and $^{\#}$4 were from WT German Landrace and POT PFFs, respectively. **e**. RT-qPCR analysis of the exogenous reprogramming factors in iPSCs either in the presence of Dox or 5 days after its removal. **f**. POT iPSCs became Td-tomato negative 5 days after Dox removal. **g**. RT-qPCR analysis of the expression of endogenous pluripotency genes in iPSCs cultured with or without Dox. **h**. Expression of lineage genes in porcine iPSCs 5-6 days after DOX removal. Gene expression was measured by RT-qPCR. Relative expression levels are shown with normalization to *GAPDH*. Experiments were performed 3 times. **i**. Diagram depicting the screen strategy for identifying culture conditions for porcine pluripotent stem cells using the Dox-dependent iPSC. Small molecule inhibitors and cytokines were selected for various combinations. Cell survival, cell morphology, and expression of endogenous *OCT4* and *NANOG* were employed as the read-outs. **j**. Images of *OCT4-Tdtomato* reporter

(POT) iPSCs in pEPSCM without Dox. In all RT-qPCR analysis, n=3 independent experiments. All graphs represent the mean ± s.d. *P* values were computed using a two-tailed t-test. For c, f and j, the experiments were repeated independently three times with similar results. Source data are provided in Supplementary Table 1. Scale bars, 100 μm.

Figure 2. **Derivation of porcine EPSCs**. **a**. Left: Schematic diagram of establishment of the pig (*Sus Scrofa*) EPSC^{Emb} lines from German Landrace day-5 *in vivo* derived blastocysts on STO feeder cells in pEPSCM, and of pEPSC^{iPS} lines by reprogramming German Landrace PFFs and China TAIHU *OCT4-Tdtomato* knock-in reporter (POT) PFFs. Right panels: images of established EPSC lines, and a fluorescence image of Td-tomato expression in POT-pEPSC^{iPS}. Three EPSC^{Emb} lines (Male: K3 and K5; Female K1) and two pEPSC^{iPS} lines (#10, #11) were extensively tested in this study. These EPSC lines behaved similarly in gene expression and differentiation. **b**. Immunostaining detection of pluripotency factors and markers, SSEA-1 and SSEA-4, in pEPSC^{Emb} and pEPSC^{iPS}. **c**. Bisulphite sequencing analysis of CpG sites in the *OCT4* and *NANOG* promoter regions in PFFs, pEPSC^{iPS} and pEPSC^{Emb}. **d**. Gene expression in embryoid bodies (EBs, day 7) of pEPSCs^{Emb}. Expression of genes of embryonic and extra-embryonic cell lineages were assessed by RT-qPCR. Relative expression levels were normalized against *GAPDH*. n=3 independent experiments. Data are mean ± s.d. *P* values were calculated using a two-tailed t-test. Statistical source data are provided in Supplementary table 10. **e**. Tissue composition of pEPSC^{Emb} teratoma sections (H&E staining): Examples of glandular epithelium derived from endoderm (i), cartilage derived from mesoderm (ii), immature neural tissue derived from ectoderm, which forms neuroepithelial structures (iii), and large multinucleated cells reminiscent of trophoblasts (arrows in iv). **f**. PL-1,

KRT7 and SDC1 positive cells in pEPSC^{Emb} teratoma sections as revealed by immunostaining. **g**. Detection of pEPSC descendants in the brain (H2BmCherry^{+}SOX2^{+}) and the liver (H2BmCherry^{+}AFP^{+}) in chimera $^{\#}$16. H2B-mCherry and SOX2 are nuclear localised whereas AFP is a cytoplasmic protein. Boxed areas are shown in higher magnification. Arrows indicate representative cells that were donor cell descendants (mCherry^{+}). DAPI stained nuclei. Additional chimera analyses are presented in Extended Data Fig. **3e-3f**. For **a-b** and **e-g**, the experiments were repeated independently three times with similar results. Scale bars, 100 μm.

Figure 3. ***In vitro*** **generation of PGC-like cells from pEPSCs^{Emb}. a**. Induction of pPGCLC by transiently expressing *SOX17* in *NANOS3-H2BmCherry* reporter pEPSCs. The presence of H2BmCherry^{+}TNAP^{+} cells in embryoid bodies (EBs) was analysed by FACS. The experiments were repeated independently three times with similar results. **b**. RT-qPCR analysis of PGC genes in day 3 EBs following pPGCLC induction. Relative expression levels werenormalized against *GAPDH*. n=3 independent experiments. Data are mean ± s.d. *P* values were calculated using a two-tailed t-test. Statistical source data are provided in Supplementary table 10. **c**. Immunofluorescence analysis of PGC factors in the sections of EBs at day 3-4 following pPGCLC induction. The H2BmCherry^{+} cells co-expressed NANOG, OCT4, BLIMP1, TFAP2C and SOX17. DAPI stained nuclei. Experiments were performed three times. **d**. RNAseq analysis (Heat map) of sorted H2BmCherry^{+} of pPGCLC induction shows expression of genes associated with PGCs, pluripotency or somatic lineages (mesoderm, endoderm, and gonadal somatic cells). **e**. Pair-wise gene expression comparison between pEPSCs^{Emb} and pPGCLCs. Key up-regulated (red) and down-regulated (blue) genes are highlighted. **f**. Bar plot shows expression of

genes related to DNA methylation in pPGCLCs and the parental pEPSCs^{Emb}. Data were from RNAseq of sorted H2BmCherry+ of pPGCLC induction. Scale bars, 100 μm.

Figure 4. Establishment of human EPSCs. a. Images of the established H1-EPSCs or M1-EPSCs (passage 25). The experiments were repeated independently three times with similar results. **b**. Expression of pluripotency genes in H1-ESCs, H1-naïve ESCs (5i), H1-EPSCs and iPSC-EPSCs. Data are mean ± s.d. (n = 3). *P* values were computed for two-tailed t-test. **c**. EBs of H1-EPSCs to PGCLCs immunostained for SOX17, BLIMP1 and OCT4. Scale bar: 100 μm. **d**. Hierarchical clustering of gene expression (bulk RNAseq) of EPSCs, and other human pluripotent stem cells. Correlation matrix was clustered using Spearman correlation and complete linkage. Data sets are: pEPSC^{Par}: porcine parthenogenetic EPSCs. E14 and AB2-EPSCs: mouse EPSCs (ref. 1); Human primed ESCs (WIBR1, iPS_NPC_4 and iPS_NPC_13) and naïve ESCs (WIBR2, WIBR3_cl_12, WIBR3_cl_16, WIN1_1 and WIN1_2) (Ref. 7 and 35); Human primed H1 ES cell (H1-rep1 and H1-rep2) and extended pluripotent stem (EPS) cells (H1_EPS_rep1, H1_EPS_rep2, ES1_EPS_rep1 and ES1_EPS_rep2) (ref. 36). **e**. Principal component analysis (PCA) of bulk RNA-seq data of EPSCs, human primed and naïve ESCs, and PFFs. Human naïve (n=5), human primed (n=3), H1-EPSC (n=2), hiPSC-EPSC (n=2), pEPSC^{Emb} (n=2), pEPSC^{iPS} (n=2), pEPSC^{Par} (n=2), PFF (n=2), E14_EPSC (n=2) and AB2_EPSC (n=1). n= biologically independent experiments. f. Pair-wise comparison of gene expression between H1-ESCs and H1-EPSCs, showing the highly expressed genes (>8 folds) in hEPSCs (total 76, red dots) and representative histone genes (blue dots). **g**. Heatmap showing expression of selected histone genes in human ESCs, EPSCs and preimplantation embryos. RNAseq data of human ESCs were from ref. 35, whereas

embryo cell data were from ref. 37. **h**. RT-qPCR analysis of four histone 1 cluster genes in seven human ESC or iPSC lines cultured under three conditions. hiPSC lines were from the HIPSC project (http://www.hipsci.org): #1, HPSI1113i-bima_1; #2, HPSI1113i-qolg_3; #3, HPSI1113i-oaaz_2; #4, HPSI1113i-uofv_1. Relative expression levels are shown with normalization to *GAPDH*. n = 3 independent experiments. Data are mean ± s.d. $^{*}P$ <0.01 compared with the FGF condition cultured cells. $^{\#}P$ <0.01 compared with 5i condition cultured cells. Experiments were performed three times. Statistical source data and precise *P* values are provided in Supplementary table 10.

Figure 5. Molecular features of porcine and human EPSC. a. Violin plots show the distribution and the probability density the scRNAseq expression of pluripotency genes in pEPSCs^{Emb} (top panel, n=150) and human H1-EPSCs (lower panel, n=96). n represents the number of cells in each plot. **b**. PCA of global gene expression pattern (by scRNAseq) of pEPSCs^{Emb} (left panel, n=150) and H1-EPSCs (right panel, n=96). n represents the number of cells in each plot. **c**. PCA and comparison of gene expression assessed by scRNAseq of human H1-EPSCs and human preimplantation embryos (ref. 39). H1-EPSCs (n=96), oocyte (n=3), zygote (n=3), 2 cell (n=6), 4 cell (n=12), 8 cell (n=20), morulae (n=16), Late blastocyst (n=30). **d**. ChIP-seq analysis of H3K27me3 and H3K4me3 marks at pluripotency gene loci in pEPSCs^{Emb} and human H1-EPSCs. **e.** Histone modifications (H3K4me3 and H3K27me3) at the loci for genes encoding enzymes involved in DNA methylation and demethylation and for cell lineage genes. For **d** and **e**, experiments were performed three times with similar results.

Figure 6. The requirement of individual components in EPSCM. a-b. Gene

expression in pEPSCs^{Emb} (**a**) and H1-EPSCs (**b**) analysed by RT-qPCR. "-SRCi, -XAV939, -ACTIVIN, -Vc, -CHIR99": removing individually; "+TGFBi, +H-CHIR99, +PD03": adding SB431542, 3.0 μM CHIR99021, or MEK1/2 inhibitor PD0325901, respectively. "WH04/A419": replacing A419259 with another SRC inhibitor, "WH-4-23. +L-CHIR99": 0.2 μM in hEPSCM. Porcine and human EPSC media contain 0.2 μM and 1.0 μM CHIR99021, respectively. Red triangle: no cell survived. **c**. Targeting the *H2B-Venus* cassette to the *OCT4* last coding exon in H1-EPSCs with the stop codon TGA being deleted. Five of 19 colonies genotyped were correctly targeted. **d**. The effects of removing WH-4-023 (-SRCi) or XAV939 (-XAV) for 7 days assessed by Venus^{+} reporter by fluorescence microscopy and flow cytometry. **e**. Western blot analysis of AXIN1 and phosphorylation of SMAD2/3 in EPSCs. EPSCs had higher levels of AXIN1 and pSMAD2/3 (for TGFβ signalling) than the differentiated (D) EPSC^{Emb} or primed H1-ESCs. **f**. TOPflash analysis for canonical Wnt signalling activity in EPSCs. Removing XAV939 (pEPSCM-X and hEPSCM-X) for 5 days increased TOPflash activity. **g**. Bright-field and immunofluorescence images showing pEPSCs^{Emb} cultured with the indicated changes in medium component. Cells were stained for OCT4 and DAPI. **h-i**. Quantitation of AP^{+} colonies formed from 2,000 pEPSCs^{Emb} (**h**) or H1-EPSCs (**i**) cultured on STO feeders with different medium components. The colonies were scored for 5 consecutive passages. -ROCKi: passaging EPSCs without the ROCK inhibitor Y27632. **j-k**. RT-qPCR analysis of the expression of lineage genes in pEPSCs^{Emb} (**j**) or hEPSCs (**k**) following removal of XAV939 or ACTIVIN A, inhibition of TGFβ signalling by SB431542, or treatment with 3.0 μM CHIR99021. **l**. The effects of supplementing 5.0 ng/ml ACTIVIN A on gene expression in EBs generated from H1-EPSCs. **m**-**n**. Effects of 5.0ng/ml ACTIVIN A on PGCLC (Tdtomato^{+}) production

from the NANOS3-Tdtomato reporter EPSCs assessed by FACS (**m**) and RT-qPCR (**n**). Relative expression levels were normalized to *GAPDH*. All graphs represent the mean ± s.d. For **a-b**, **j-l** and **n**, n = 3 independent experiments. For **f**, **h-i** and **m**, n = 4 independent experiments. For **d-e** and **g**, the experiments were repeated independently three times with similar results. *P* values were computed by two-tailed t-test. Statistical source data are presented in Supplementary table 10. Scale bars: 100 μm.

Figure 7. Trophoblast differentiation potential of hEPSCs. a. Left panel: differentiation of hEPSCs to trophoblasts under TGFβ inhibition. Right panel: flow cytometry analysis of trophoblast differentiation of *CDX2-H2B-Venus* reporter EPSCs, collected 4 days after TGFβ inhibition. The *CDX2-H2B-Venus* reporter EPSCs were also cultured in conventional FGF-containing hESCs medium or 5i-naïve medium and differentiated under TGFβ inhibition and examined by flow cytometry. The experiments were repeated independently three times with similar results. **b**. The dynamic changes in the expression of trophoblast genes during hEPSC differentiation (sampled at 2-day intervals for 12days) were assayed by RT-qPCR. Relative expression levels were normalized against *GAPDH*. n = 3 independent experiments. Data are mean ± s.d. $^{*}P$ <0.01 compared with H1-ESC cells. $^{\#}P$ <0.01 compared with H1-5i cells. The precise *P* values are presented in Supplementary table 10. **c**. tSNE analysis of RNA-seq data of the differentiating human ESCs (n = 2) and iPSC-EPSCs (n = 4) treated with TGFβ inhibitor SB431542. RNAs were sampled from cells at Day 0-12 of differentiation. The of H1-EPSCs and hiPSC-EPSCs showed different trajectory of differentiation from H1-ESCs. **d**. Heatmap shows changes in the expression of trophoblast-specific genes in differentiating H1-ESCs (green), H1-EPSCs (red) and iPSC-EPSCs (blue) collected at several time points of culture for RNAseq analysis. **e**. DNA demethylation at the promoter region of the *ELF5* locus in

differentiating H1-EPSCs and other cell types following 6 days of SB431542 treatment. Cells from H1-ESCs, H1-naïve ESCs (5i) showed no discernible DNA demethylation at the *ELF5* promoter. **f**. Secreted hormones from trophoblasts derived from H1-EPSCs induced by TGFβ inhibition (SB431542). VEGF, PLGF, sFlt-1and sEng were measured in the conditioned media for culturing the differentiating EPSCs or ESCs for 16 days following a 48-h SB431542 treatment. **g**. hCG produced by trophoblasts from SB431542-treated EPSCs or ESCs at day 10 of differentiation, measured by ELISA. n = 4 independent experiments. Data are mean ± s.d. *P* values were calculated using a two-tailed t-test. Statistical source data are presented in Supplementary table 10.

Figure 8. Derivation of trophoblast stem cell-like cells from hEPSCs. a. Phase-contrast images of primary TSC colonies formed from individual hEPSCs (left) and of TSCs at passage 7 (right). **b**. Expression of trophoblast markers GATA3, TFAP2C and KRT7 in EPSC-TSCs detected by immunostaining. Nuclei were stained with DAPI. Similar results were obtained with four independent EPSC-TSC lines. **c**. RT-qPCR analysis of pluripotency and TSC genes in four EPSC-derived TSC lines and their parental hEPSCs. JEG3 and JAR are trophoblast cell lines. n = 3 independent experiments. Data are mean ± s.d.. *$p < 0.01$ compared to TSCs. The precise *P* values are presented in Supplementary table 10. **d**. PCA of gene expression of hTSCs (n = 3) and of cells differentiated from human EPSCs (n = 2) under TGFβ inhibition at several time points. hTSCs showed enriched transcriptomic features of day-4 differentiated EPSCs. **e**. Immunostaining of SDC1 and CGB in hTSC-dervied syncytiotrophoblasts. DAPI stained the nucleus. **f**. Phase-contrast and Hoechst staining images of multinucleated hTSC-derived syncytiotrophoblasts. **g**. The fusion index of forming syncytiotrophoblasts from hTSCs calculated as the number of nuclei

in syncytia/total number of nuclei. n = 4 independent experiments. Data are mean ± s.d. **h**. RT-qPCR analysis of trophoblast-specific genes in syncytiotrophoblast (ST) and extravillous trophoblast (EVT) derived from three hTSC lines. Expression levels were normalized against *GAPDH*. n = 3 independent experiments. Data are mean ± s.d. **i**. Flow cytometry detection of HLA-ABC and HLA-G in hESCs, hEPSCs, hTSCs, and hTSC-derived EVT cells (protocol of ref. 46). The choriocarcinoma cells JEG-3 and JAR represent the extravillous and villous trophoblast cells, respectively. JEG-3 cells expressed HLA-G, HLA-C and HLA-E, but not JAR cells. **j**. H&E staining of lesions formed by hTSCs engrafted subcutaneously in NOD-SCID mice. **k**. Confocal images of immunostaining for SDC1- or KRT7-positive cells in hTSC-derived lesions. DAPI stained the nucleus. **l**. Serum hCG levels in six NOD-SCID mice 7 days after hTSC engraftment (n = 3) or injection of vehicle only (n = 3). For **a-b**, **e-f** and **h-l**, the experiments were repeated independently three times with similar results. Statistical source data are presented in Supplementary table 10. Scale bars: 100 μm.

Figure 1

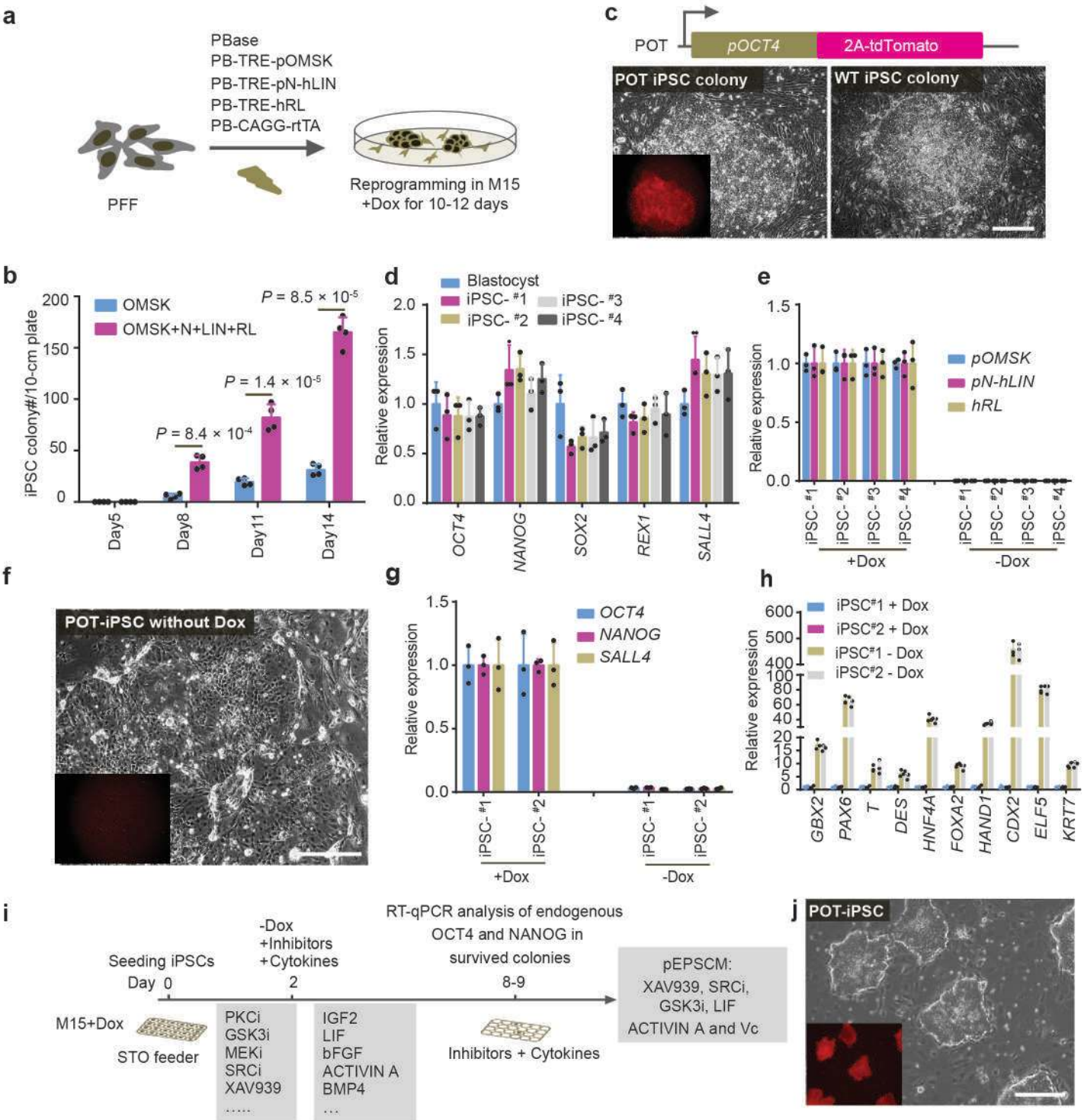
a
PBase
PB-TRE-pOMSK
PB-TRE-pN-hLIN
PB-TRE-hRL
PB-CAGG-rtTA
PFF
Reprogramming in M15
+Dox for 10-12 days
c
POT
pOCT4
2A-tdTomato
POT iPSC colony
WT iPSC colony
b
iPSC colony#/10-cm plate
OMSK
OMSK+N+LIN+RL
P = 8.5 × 10-5
P = 1.4 × 10-5
P = 8.4 × 10-4
Day5
Day8
Day11
Day14
d
Blastocyst
iPSC- #1
iPSC- #2
iPSC- #3
iPSC- #4
Relative expression
OCT4
NANOG
SOX2
REX1
SALL4
e
pOMSK
pN-hLIN
hRL
+Dox
-Dox
f
POT-iPSC without Dox
g
OCT4
NANOG
SALL4
h
iPSC#1 + Dox
iPSC#2 + Dox
iPSC#1 - Dox
iPSC#2 - Dox
GBX2
PAX6
T
DES
HNF4A
FOXA2
HAND1
CDX2
ELF5
KRT7
i
Seeding iPSCs
Day 0
-Dox
+Inhibitors
+Cytokines
2
RT-qPCR analysis of endogenous
OCT4 and NANOG in
survived colonies
8-9
M15+Dox
STO feeder
PKCi
GSK3i
MEKi
SRCi
XAV939
IGF2
LIF
bFGF
ACTIVIN A
BMP4
Inhibitors + Cytokines
pEPSCM:
XAV939, SRCi,
GSK3i, LIF
ACTIVIN A and Vc
j
POT-iPSC

Figure 2

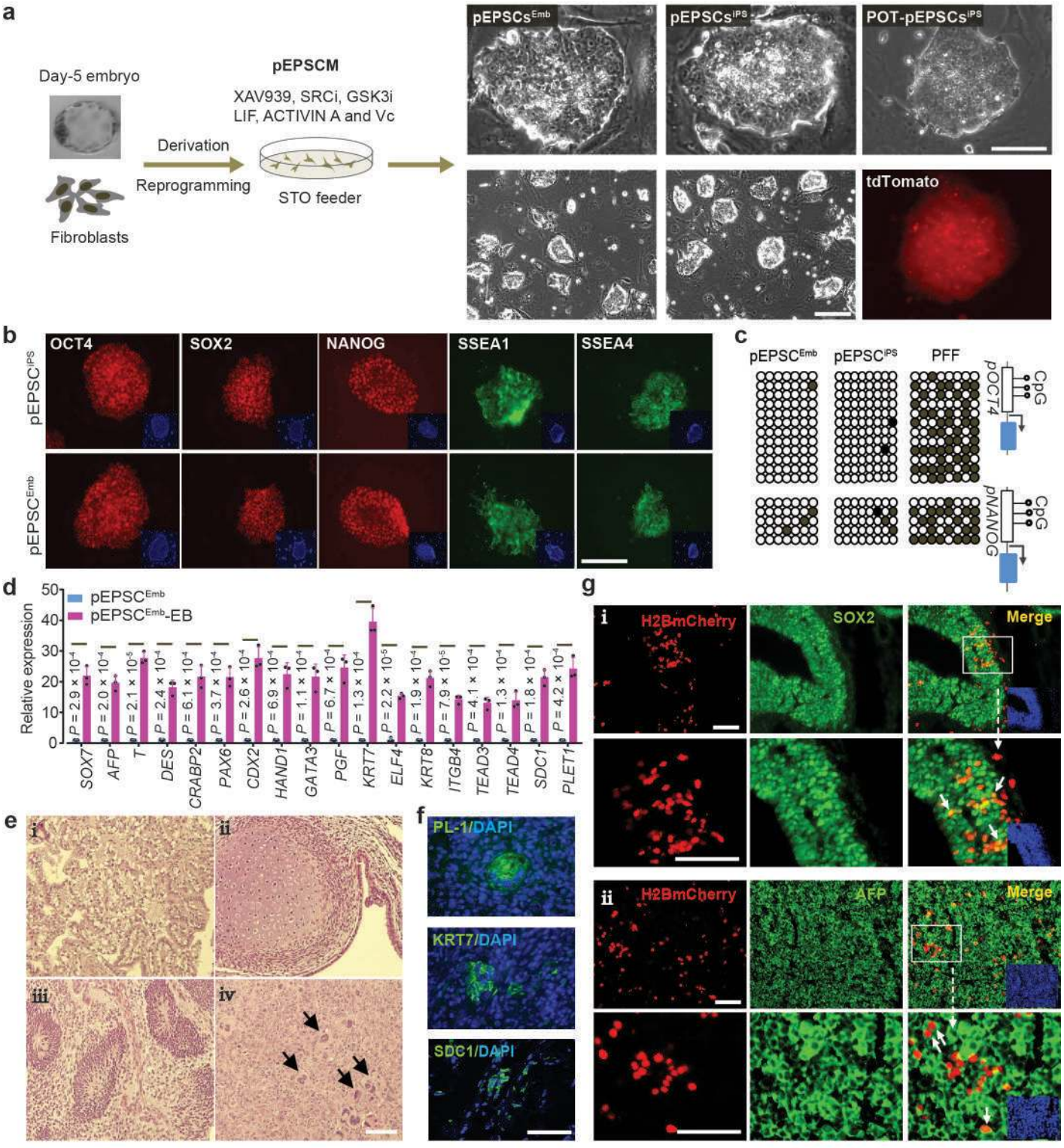
a
Day-5 embryo
Fibroblasts
Derivation
Reprogramming
pEPSCM
XAV939, SRCi, GSK3i
LIF, ACTIVIN A and Vc
STO feeder
pEPSCs^Emb
pEPSCs^IPS
POT-pEPSCs^IPS
tdTomato
b
OCT4
SOX2
NANOG
SSEA1
SSEA4
pEPSC^IPS
pEPSC^Emb
c
pEPSC^Emb
pEPSC^IPS
PFF
pOCT4
pNANOG
CpG
d
pEPSC^Emb
pEPSC^Emb-EB
Relative expression
SOX7
AFP
T
DES
CRABP2
PAX6
CDX2
HAND1
GATA3
PGF
KRT7
ELF4
KRT8
ITGB4
TEAD3
TEAD4
SDC1
PLET1
e
i
ii
iii
iv
f
PL-1/DAPI
KRT7/DAPI
SDC1/DAPI
g
i
H2BmCherry
SOX2
Merge
ii
H2BmCherry
AFP
Merge

Figure 3

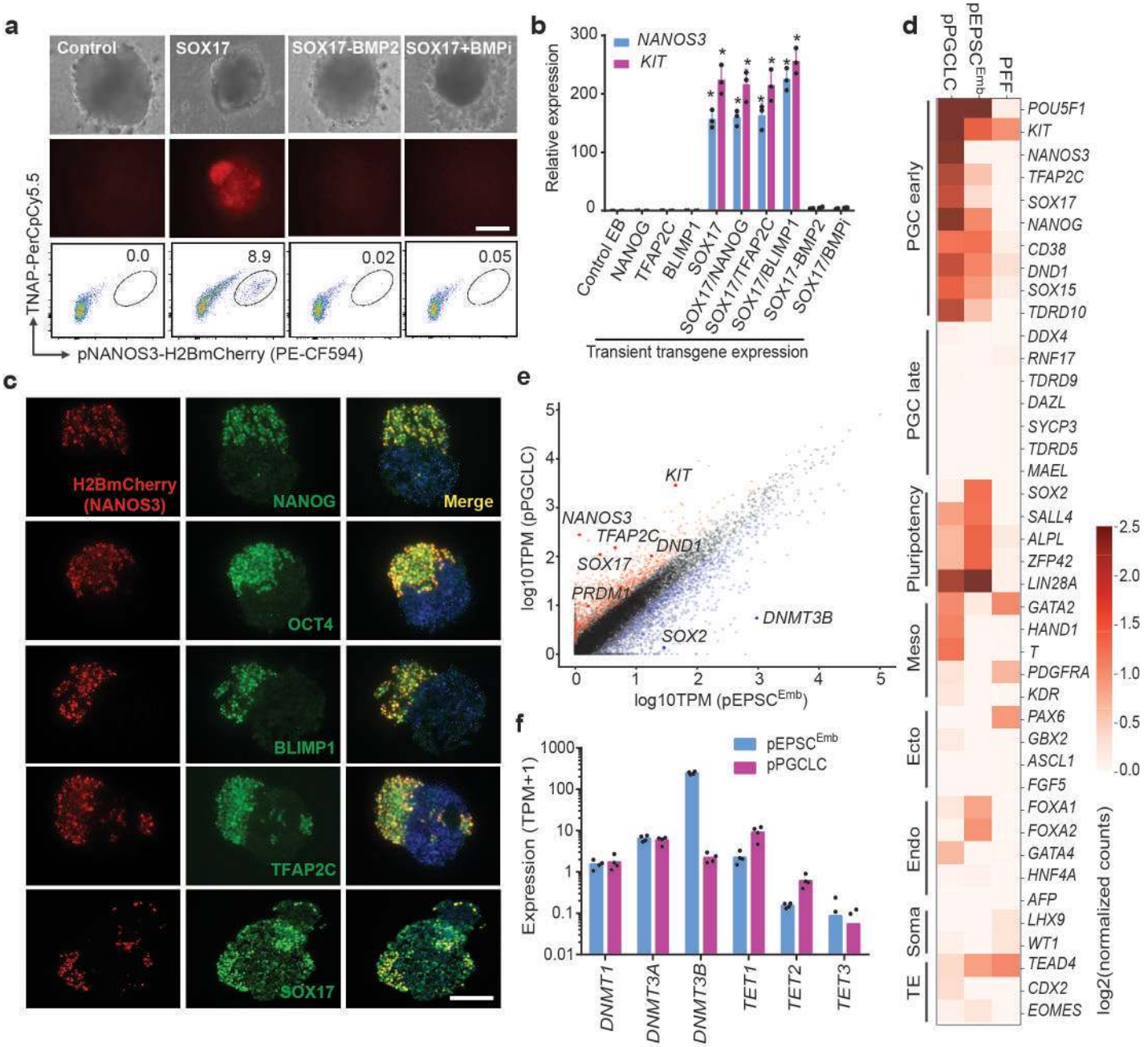
a
Control
SOX17
SOX17-BMP2
SOX17+BMPi
TNAP-PerCpCy5.5
0.0
8.9
0.02
0.05
pNANOS3-H2BmCherry (PE-CF594)
b
NANOS3
KIT
Relative expression
300
200
100
0
Control EB
NANOG
TFAP2C
BLIMP1
SOX17
SOX17/NANOG
SOX17/TFAP2C
SOX17/BLIMP1
SOX17-BMP2
SOX17/BMPi
Transient transgene expression
c
H2BmCherry (NANOS3)
NANOG
Merge
OCT4
BLIMP1
TFAP2C
SOX17
d
pPGCLC
pEPSC^Emb
PFF
POU5F1
KIT
NANOS3
TFAP2C
SOX17
NANOG
CD38
DND1
SOX15
TDRD10
DDX4
RNF17
TDRD9
DAZL
SYCP3
TDRD5
MAEL
SOX2
SALL4
ALPL
ZFP42
LIN28A
GATA2
HAND1
T
PDGFRA
KDR
PAX6
GBX2
ASCL1
FGF5
FOXA1
FOXA2
GATA4
HNF4A
AFP
LHX9
WT1
TEAD4
CDX2
EOMES
PGC early
PGC late
Pluripotency
Meso
Ecto
Endo
Soma
TE
log2(normalized counts)
2.5
2.0
1.5
1.0
0.5
0.0
e
log10TPM (pPGCLC)
log10TPM (pEPSC^Emb)
KIT
NANOS3
TFAP2C
DND1
SOX17
PRDM1
DNMT3B
SOX2
f
Expression (TPM+1)
1000
100
10
1
0.1
0.01
pEPSC^Emb
pPGCLC
DNMT1
DNMT3A
DNMT3B
TET1
TET2
TET3

Figure 4

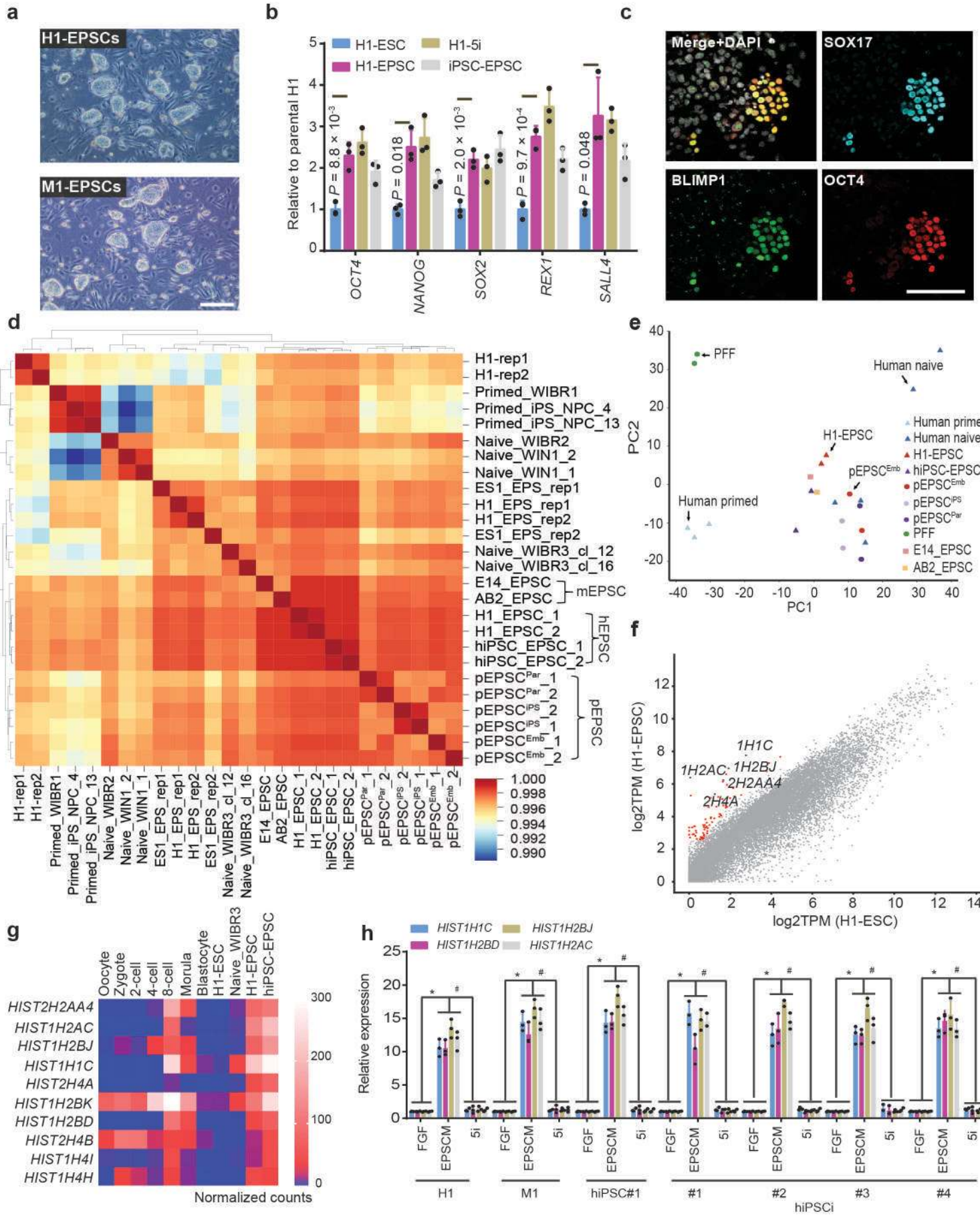
a
H1-EPSCs
M1-EPSCs
b
H1-ESC
H1-5i
H1-EPSC
iPSC-EPSC
Relative to parental H1
P = 8.8 × 10-3
P = 0.018
P = 2.0 × 10-3
P = 9.7 × 10-4
P = 0.048
OCT4
NANOG
SOX2
REX1
SALL4
c
Merge+DAPI
SOX17
BLIMP1
OCT4
d
H1-rep1
H1-rep2
Primed_WIBR1
Primed_iPS_NPC_4
Primed_iPS_NPC_13
Naive_WIBR2
Naive_WIN1_2
Naive_WIN1_1
ES1_EPS_rep1
H1_EPS_rep1
H1_EPS_rep2
ES1_EPS_rep2
Naive_WIBR3_cl_12
Naive_WIBR3_cl_16
E14_EPSC
AB2_EPSC
mEPSC
H1_EPSC_1
H1_EPSC_2
hiPSC_EPSC_1
hiPSC_EPSC_2
hEPSC
pEPSCPar_1
pEPSCPar_2
pEPSCiPS_2
pEPSCiPS_1
pEPSCEmb_1
pEPSCEmb_2
pEPSC
1.000
0.998
0.996
0.994
0.992
0.990
e
PFF
Human naive
H1-EPSC
pEPSCEmb
Human primed
PC2
PC1
Human primed
Human naive
H1-EPSC
hiPSC-EPSC
pEPSCEmb
pEPSCiPS
pEPSCPar
PFF
E14_EPSC
AB2_EPSC
f
1H1C
1H2AC
1H2BJ
2H2AA4
2H4A
log2TPM (H1-EPSC)
log2TPM (H1-ESC)
g
Oocyte
Zygote
2-cell
4-cell
8-cell
Morula
Blastocyte
H1-ESC
Naive_WIBR3
H1-EPSC
hiPSC-EPSC
HIST2H2AA4
HIST1H2AC
HIST1H2BJ
HIST1H1C
HIST2H4A
HIST1H2BK
HIST1H2BD
HIST2H4B
HIST1H4I
HIST1H4H
300
200
100
0
Normalized counts
h
HIST1H1C
HIST1H2BJ
HIST1H2BD
HIST1H2AC
Relative expression
FGF
EPSCM
5i
H1
M1
hiPSC#1
#1
#2
#3
#4
hiPSCi

Figure 5

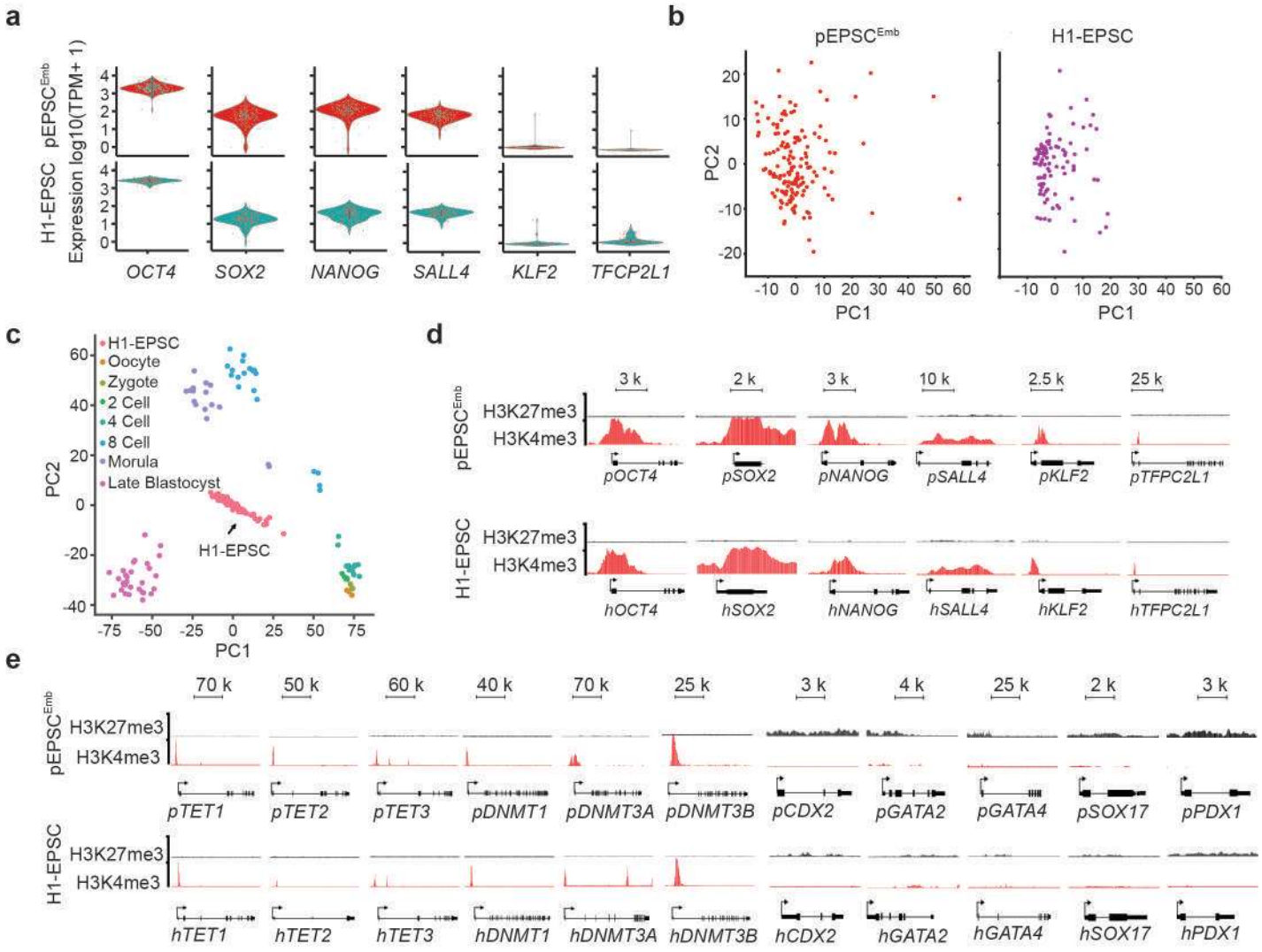
a
pEPSC^Emb
H1-EPSC
Expression log10(TPM+ 1)
OCT4
SOX2
NANOG
SALL4
KLF2
TFCP2L1
b
pEPSC^Emb
H1-EPSC
PC2
PC1
c
H1-EPSC
Oocyte
Zygote
2 Cell
4 Cell
8 Cell
Morula
Late Blastocyst
PC2
PC1
d
pEPSC^Emb
H1-EPSC
H3K27me3
H3K4me3
pOCT4
pSOX2
pNANOG
pSALL4
pKLF2
pTFPC2L1
hOCT4
hSOX2
hNANOG
hSALL4
hKLF2
hTFPC2L1
e
pEPSC^Emb
H1-EPSC
H3K27me3
H3K4me3
pTET1
pTET2
pTET3
pDNMT1
pDNMT3A
pDNMT3B
pCDX2
pGATA2
pGATA4
pSOX17
pPDX1
hTET1
hTET2
hTET3
hDNMT1
hDNMT3A
hDNMT3B
hCDX2
hGATA2
hGATA4
hSOX17
hPDX1

Figure 6

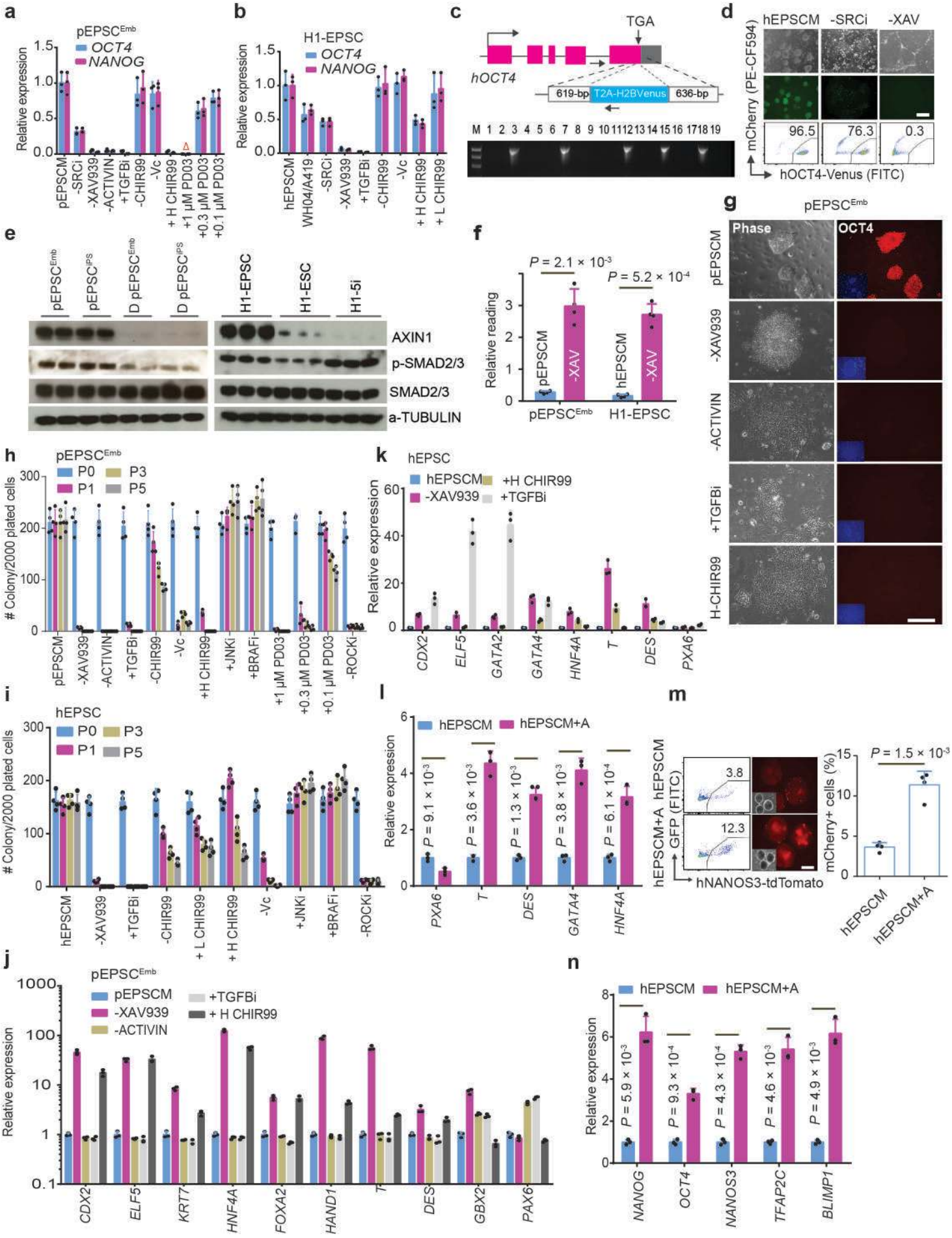
a
pEPSC^Emb
OCT4
NANOG
Relative expression
pEPSCM
-SRCi
-XAV939
-ACTIVIN
+TGFBi
-CHIR99
-Vc
+ H CHIR99
+1 μM PD03
+0.3 μM PD03
+0.1 μM PD03
b
H1-EPSC
OCT4
NANOG
Relative expression
hEPSCM
WH04/A419
-SRCi
-XAV939
+TGFBi
-CHIR99
-Vc
+ H CHIR99
+ L CHIR99
c
TGA
hOCT4
619-bp
T2A-H2BVenus
636-bp
M 1 2 3 4 5 6 7 8 9 10 11 12 13 14 15 16 17 18 19
d
hEPSCM
-SRCi
-XAV
mCherry (PE-CF594)
96.5
76.3
0.3
hOCT4-Venus (FITC)
e
pEPSC^Emb
pEPSC^iPS
D pEPSC^Emb
D pEPSC^iPS
H1-EPSC
H1-ESC
H1-5i
AXIN1
p-SMAD2/3
SMAD2/3
a-TUBULIN
f
P = 2.1 × 10^-3
P = 5.2 × 10^-4
Relative reading
pEPSCM
-XAV
hEPSCM
-XAV
pEPSC^Emb
H1-EPSC
g
pEPSC^Emb
Phase
OCT4
pEPSCM
-XAV939
-ACTIVIN
+TGFBi
H-CHIR99
h
pEPSC^Emb
P0
P1
P3
P5
Colony/2000 plated cells
pEPSCM
-XAV939
-ACTIVIN
+TGFBi
-CHIR99
-Vc
+H CHIR99
+JNKi
+BRAFi
+1 μM PD03
+0.3 μM PD03
+0.1 μM PD03
-ROCKi
k
hEPSC
hEPSCM
+H CHIR99
-XAV939
+TGFBi
Relative expression
CDX2
ELF5
GATA2
GATA4
HNF4A
T
DES
PXA6
i
hEPSC
P0
P1
P3
P5
Colony/2000 plated cells
hEPSCM
-XAV939
+TGFBi
-CHIR99
+ L CHIR99
+ H CHIR99
-Vc
+JNKi
+BRAFi
-ROCKi
l
hEPSCM
hEPSCM+A
Relative expression
P = 9.1 × 10^-3
P = 3.6 × 10^-3
P = 1.3 × 10^-3
P = 3.8 × 10^-3
P = 6.1 × 10^-4
PXA6
T
DES
GATA4
HNF4A
m
hEPSCM
hEPSCM+A
GFP (FITC)
3.8
12.3
hNANOS3-tdTomato
mCherry+ cells (%)
P = 1.5 × 10^-3
hEPSCM
hEPSCM+A
j
pEPSC^Emb
pEPSCM
-XAV939
-ACTIVIN
+TGFBi
+ H CHIR99
Relative expression
CDX2
ELF5
KRT7
HNF4A
FOXA2
HAND1
T
DES
GBX2
PAX6
n
hEPSCM
hEPSCM+A
Relative expression
P = 5.9 × 10^-3
P = 9.3 × 10^-4
P = 4.3 × 10^-4
P = 4.6 × 10^-3
P = 4.9 × 10^-3
NANOG
OCT4
NANOS3
TFAP2C
BLIMP1

Figure 7

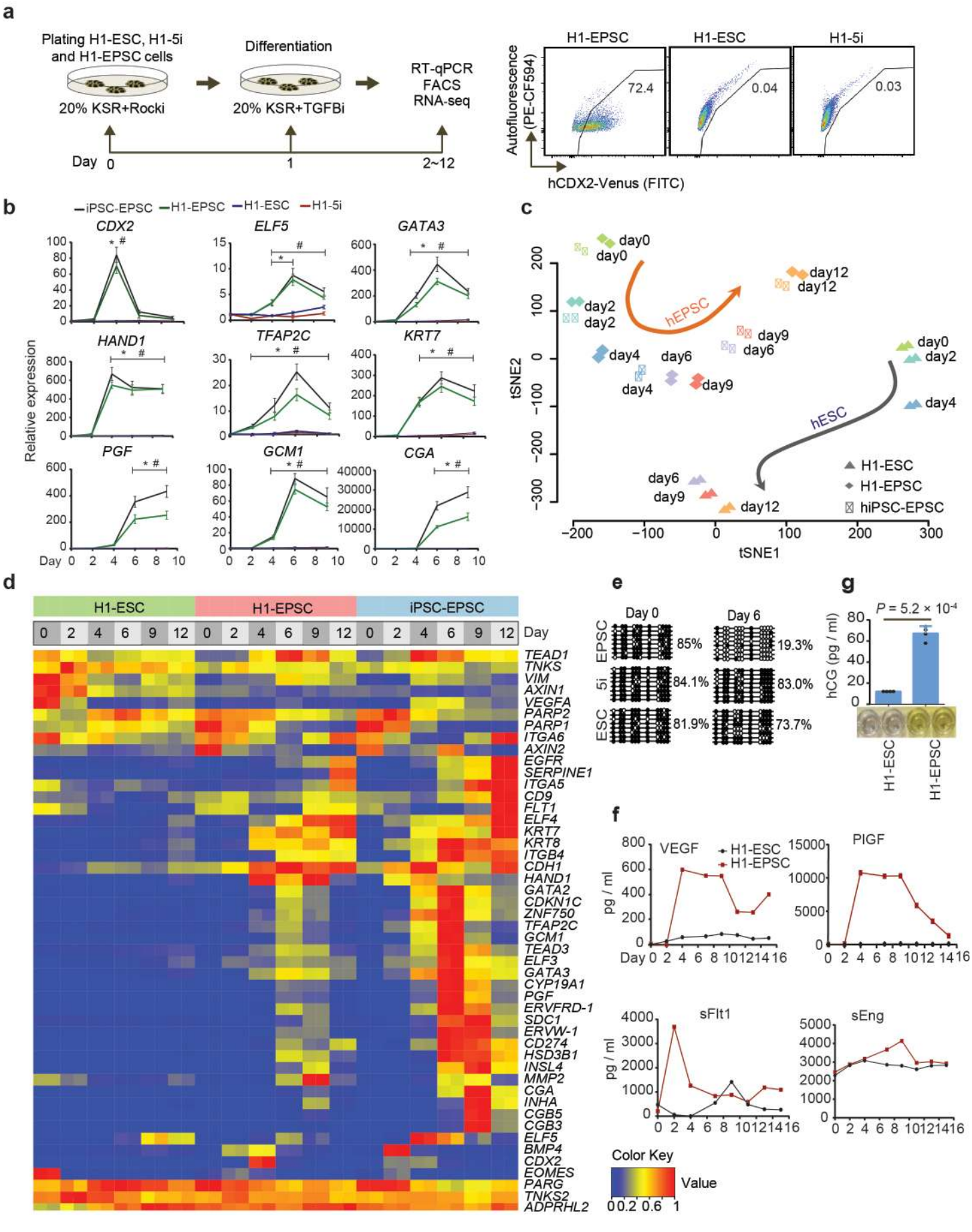
a
Plating H1-ESC, H1-5i and H1-EPSC cells
20% KSR+Rocki
Differentiation
20% KSR+TGFBi
RT-qPCR
FACS
RNA-seq
Day 0
1
2~12
H1-EPSC
H1-ESC
H1-5i
72.4
0.04
0.03
Autofluorescence (PE-CF594)
hCDX2-Venus (FITC)
b
iPSC-EPSC
H1-EPSC
H1-ESC
H1-5i
CDX2
ELF5
GATA3
HAND1
TFAP2C
KRT7
PGF
GCM1
CGA
Relative expression
Day
c
hEPSC
hESC
tSNE1
tSNE2
H1-ESC
H1-EPSC
hiPSC-EPSC
d
H1-ESC
H1-EPSC
iPSC-EPSC
Day
TEAD1
TNKS
VIM
AXIN1
VEGFA
PARP2
PARP1
ITGA6
AXIN2
EGFR
SERPINE1
ITGA5
CD9
FLT1
ELF4
KRT7
KRT8
ITGB4
CDH1
HAND1
GATA2
CDKN1C
ZNF750
TFAP2C
GCM1
TEAD3
ELF3
GATA3
CYP19A1
PGF
ERVFRD-1
SDC1
ERVW-1
CD274
HSD3B1
INSL4
MMP2
CGA
INHA
CGB5
CGB3
ELF5
BMP4
CDX2
EOMES
PARG
TNKS2
ADPRHL2
e
Day 0
Day 6
EPSC
5i
ESC
85%
19.3%
84.1%
83.0%
81.9%
73.7%
g
P = 5.2 × 10-4
hCG (pg / ml)
H1-ESC
H1-EPSC
f
VEGF
PIGF
sFlt1
sEng
pg / ml
Color Key
Value

Figure 8

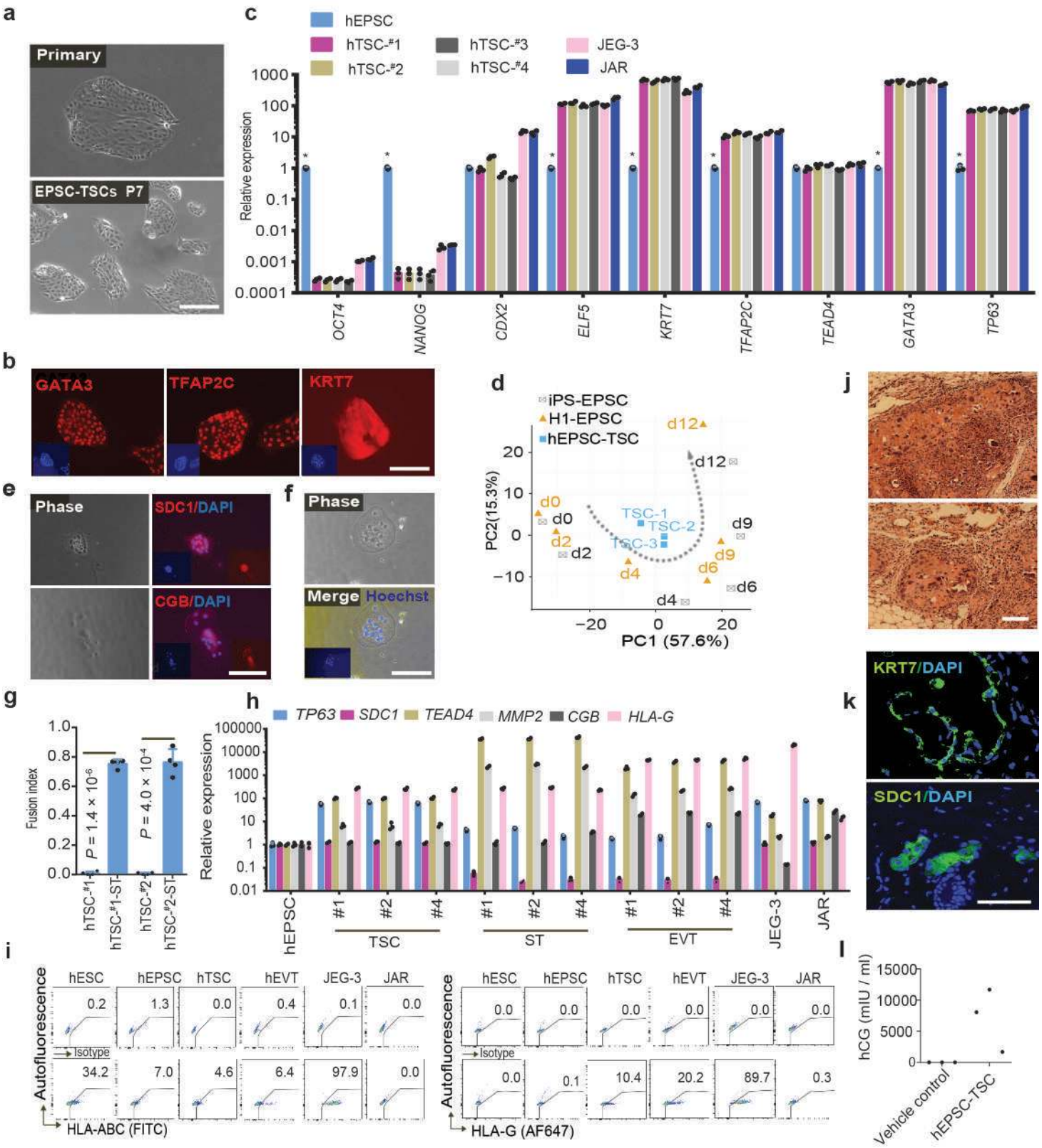
a
Primary
EPSC-TSCs P7
c
hEPSC
hTSC-#1
hTSC-#2
hTSC-#3
hTSC-#4
JEG-3
JAR
Relative expression
OCT4
NANOG
CDX2
ELF5
KRT7
TFAP2C
TEAD4
GATA3
TP63
b
GATA3
TFAP2C
KRT7
d
iPS-EPSC
H1-EPSC
hEPSC-TSC
PC2(15.3%)
PC1 (57.6%)
TSC-1
TSC-2
TSC-3
e
Phase
SDC1/DAPI
CGB/DAPI
f
Phase
Merge Hoechst
j
k
KRT7/DAPI
SDC1/DAPI
g
Fusion index
P = 1.4 × 10-6
P = 4.0 × 10-4
hTSC-#1
hTSC-#1-ST
hTSC-#2
hTSC-#2-ST
h
TP63 SDC1 TEAD4 MMP2 CGB HLA-G
Relative expression
hEPSC
TSC
ST
EVT
JEG-3
JAR
i
hESC
hEPSC
hTSC
hEVT
JEG-3
JAR
Isotype
Autofluorescence
HLA-ABC (FITC)
HLA-G (AF647)
l
hCG (mIU / ml)
Vehicle control
hEPSC-TSC

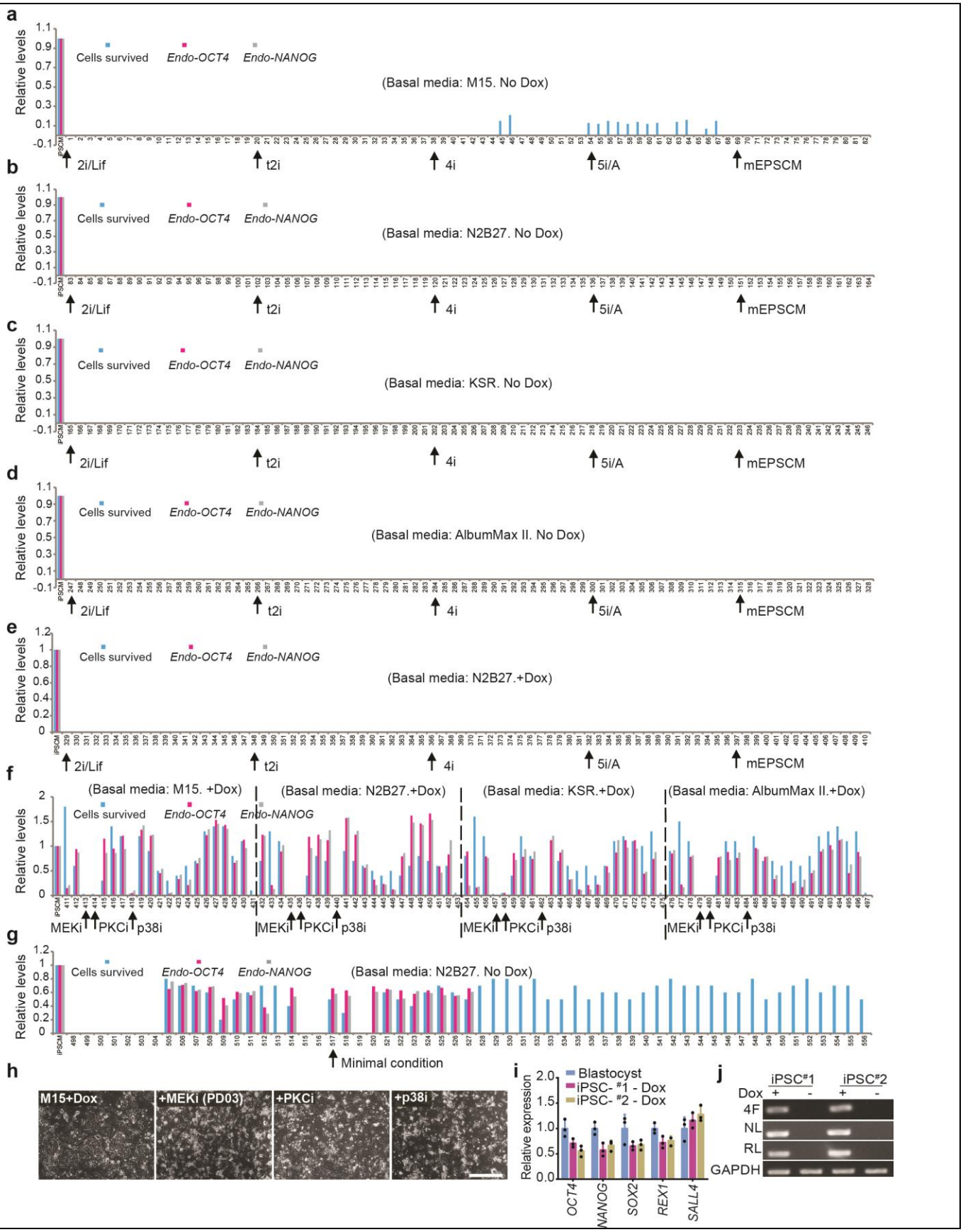
a
b
c
d
e
f
g
h
i
j
Relative levels
Cells survived
Endo-OCT4
Endo-NANOG
(Basal media: M15. No Dox)
(Basal media: N2B27. No Dox)
(Basal media: KSR. No Dox)
(Basal media: AlbumMax II. No Dox)
(Basal media: N2B27.+Dox)
(Basal media: M15. +Dox)
(Basal media: N2B27.+Dox)
(Basal media: KSR.+Dox)
(Basal media: AlbumMax II.+Dox)
2i/Lif
t2i
4i
5i/A
mEPSCM
MEKi
PKCi
p38i
Minimal condition
M15+Dox
+MEKi (PD03)
+PKCi
+p38i
Relative expression
Blastocyst
iPSC- #1 - Dox
iPSC- #2 - Dox
OCT4
NANOG
SOX2
REX1
SALL4
iPSC#1
iPSC#2
Dox
4F
NL
RL
GAPDH

Supplementary Figure 1

Culture condition screening for porcine EPSC

a-g. The relative expression levels of endogenous *OCT4* and *NANOG* in the survived cells after 6 days of culture in different basal media supplemented with inhibitors and cytokines combinations: **a**. M15 medium without Dox; **b**. N2B27 basal medium without Dox; **c**. 20% KOSR medium without Dox; **d**. AlbumMax II basal medium without Dox; **e**. N2B27 basal medium with Dox; **f**. Four individual basal media with Dox (M15: 411-431; N2B27: 432-453; KOSR: 454-475; AlbumMax II: 476-497); **g**. N2B27 basal medium without Dox. 2i: GSK3i and MEKi; t2i: GSK3i, MEKi and PKCi (Takashima, Y., et al. 2014 Cell); 4i: GSK3i, MEKi, JNKi and p38i (Irie, N., et al 2015 Cell); 5i: GSK3i, MEKi, ROCKi, BRAFi and SRCi (Theunissen, T. W., et al. 2014 Cell Stem Cell); mEPSCM: GSK3i, MEKi, JNKi, XAV939, SRCi and p38i (Yang J., et al. 2017 Nature); Details of the inhibitor combinations are presented in Supplementary Table 1. Relative expression levels were normalized to *GAPDH*. **h**. Images showing the toxicity of MEKi, PKCi and p38i to the porcine iPSCs in M15 plus Dox. **i**. Endogenous pluripotency gene expression in porcine iPSCs in the absence of Dox in pEPSCM (#517 minimal condition, Extended Data Fig. 2h). Gene expression was compared to that of porcine blastocysts. $n = 3$ independent experiments. Data are mean ± s.d. **j**. Detection of expression of the exogenous reprogramming factors by RT-PCR showed no detectable leaky expression in about half of the iPSC lines. For **h** and **j**, the experiments were repeated independently three times with similar results. Statistical source data are presented in Supplementary Table 1 and Supplementary Table 10. Scale bar: 100 μm.

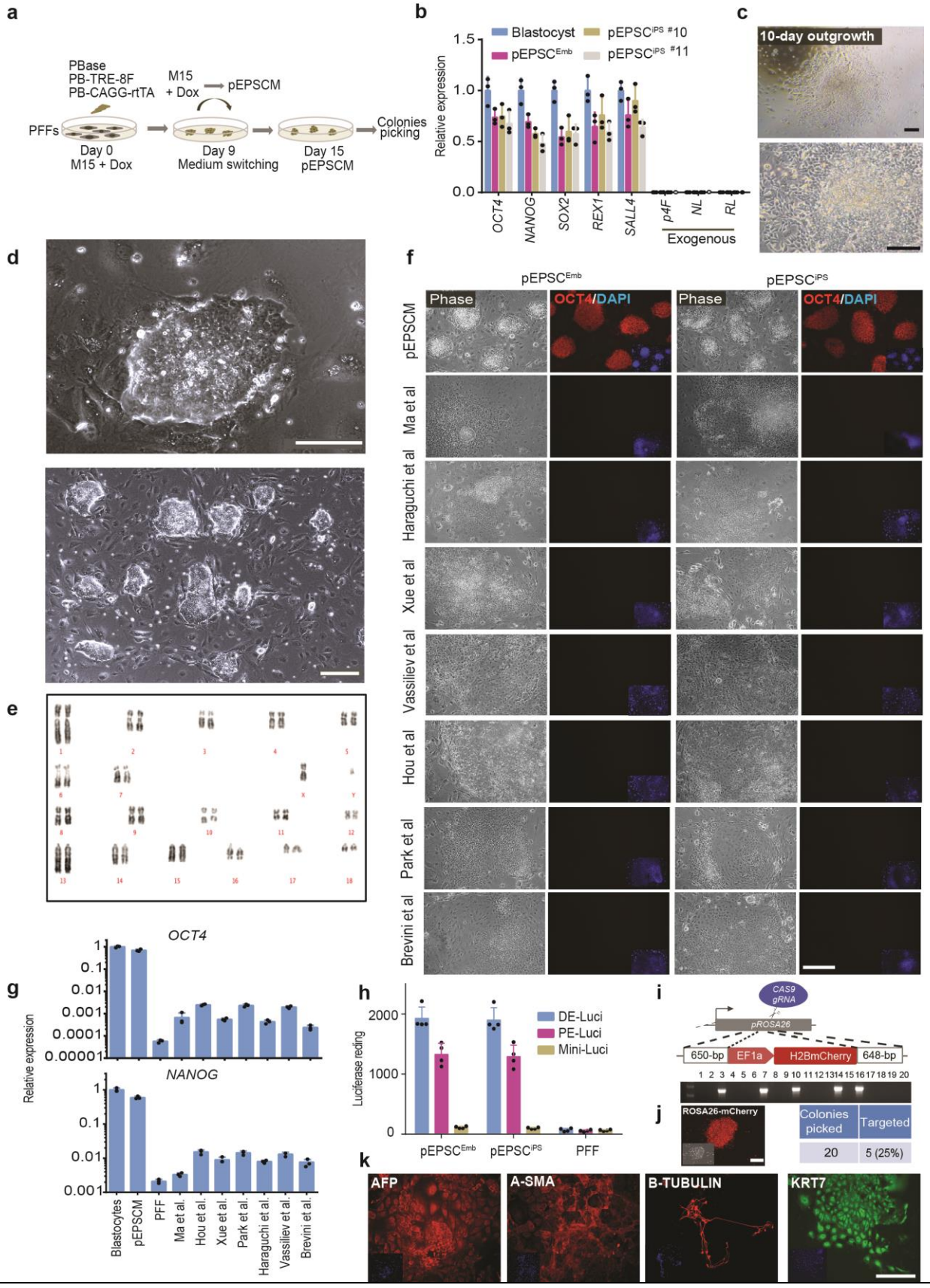
a
PBase
PB-TRE-8F
PB-CAGG-rtTA
M15
+ Dox
pEPSCM
PFFs
Day 0
M15 + Dox
Day 9
Medium switching
Day 15
pEPSCM
Colonies picking
b
Blastocyst
pEPSCEmb
pEPSCiPS #10
pEPSCiPS #11
Relative expression
1.5
1.0
0.5
0.0
OCT4
NANOG
SOX2
REX1
SALL4
p4F
NL
RL
Exogenous
c
10-day outgrowth
d
e
f
pEPSCEmb
pEPSCiPS
Phase
OCT4/DAPI
pEPSCM
Ma et al
Haraguchi et al
Xue et al
Vassiliev et al
Hou et al
Park et al
Brevini et al
g
OCT4
NANOG
Relative expression
1
0.1
0.01
0.001
0.0001
0.00001
Blastocytes
pEPSCM
PFF
Ma et al.
Hou et al.
Xue et al.
Park et al.
Haraguchi et al.
Vassiliev et al.
Brevini et al.
h
DE-Luci
PE-Luci
Mini-Luci
Luciferase reding
2000
1000
0
pEPSCEmb
pEPSCiPS
PFF
i
CAS9
gRNA
pROSA26
650-bp
EF1a
H2BmCherry
648-bp
1 2 3 4 5 6 7 8 9 10 11 12 13 14 15 16 17 18 19 20
j
ROSA26-mCherry
Colonies picked
Targeted
20
5 (25%)
k
AFP
A-SMA
B-TUBULIN
KRT7

Supplementary Figure 2

Establishment of porcine EPSCs by reprogramming PFFs or from pre-implantation embryos

a. Schematic diagram of reprogramming PFFs to establish EPSC lines in pEPSCM. **b**. Two WT pEPSC^{iPS} lines (#10 and #11) were examined for expression of endogenous pluripotency genes and the exogenous reprogramming factors. n= 3 independent experiments. Data are mean ± s.d. **c**. Day-10 outgrowth from a porcine early blastocyst in pEPSCM supplemented with a ROCK inhibitor. The outgrowths were picked at day 10-12 for dissociation and re-plating to establish stable lines. **d**. Representative images of the pEPSC^{Emb} (Line K3) established from pig *in vivo* derived embryos. Experiments were performed at least three times. **e**. pEPSC^{Emb} (Line K3) retained a normal karyotype after 25 passages (10/10 metaphase spreads examined were normal). Two additional lines examined also maintained the normal karyotype after more than 25 passages. **f-g**. pEPSCs were cultured under seven previously reported porcine ESCs conditions for 7 days, and cell morphology and gene expression were examined. **f**. Immunofluorescence staining for OCT4 expression. **g**. RT-qPCR detection of *OCT4* and *NANOG* in pEPSCs. n = 3 independent experiments. Data are mean ± s.d. **h**. Active *Oct4* distal enhancer in porcine EPSC^{Emb} and EPSC^{iPS}. The mouse *Oct4* distal and proximal enhancer constructs were used in the luciferase assay. n = 4 independent experiments. Data are mean ± s.d. **i**. Genome-editing in pEPSCs^{Emb}: Knocking-in the *H2B-mCherry* expressing cassette into pig *ROSA26* locus by Crispr/Cas9. 5 out 20 colonies picked for genotyping were correctly targeted and retained a normal karyotype. **j**. Bright field and fluorescence images of the pEPSC^{Emb} colonies with the *H2B-mCherry* correctly targeted to the *ROSA26* locus. **k.** *in vitro* differentiation of pEPSC^{Emb} to cells of the germ layers and the trophectoderm lineage (KRT7^{+}). Relative expression levels were normalized to *GAPDH*. For **c**, **f** and **i-k**, the experiments were repeated independently three times with similar results. Statistical source data are provided in Supplementary Table 10. Scale bars: 100 μm.

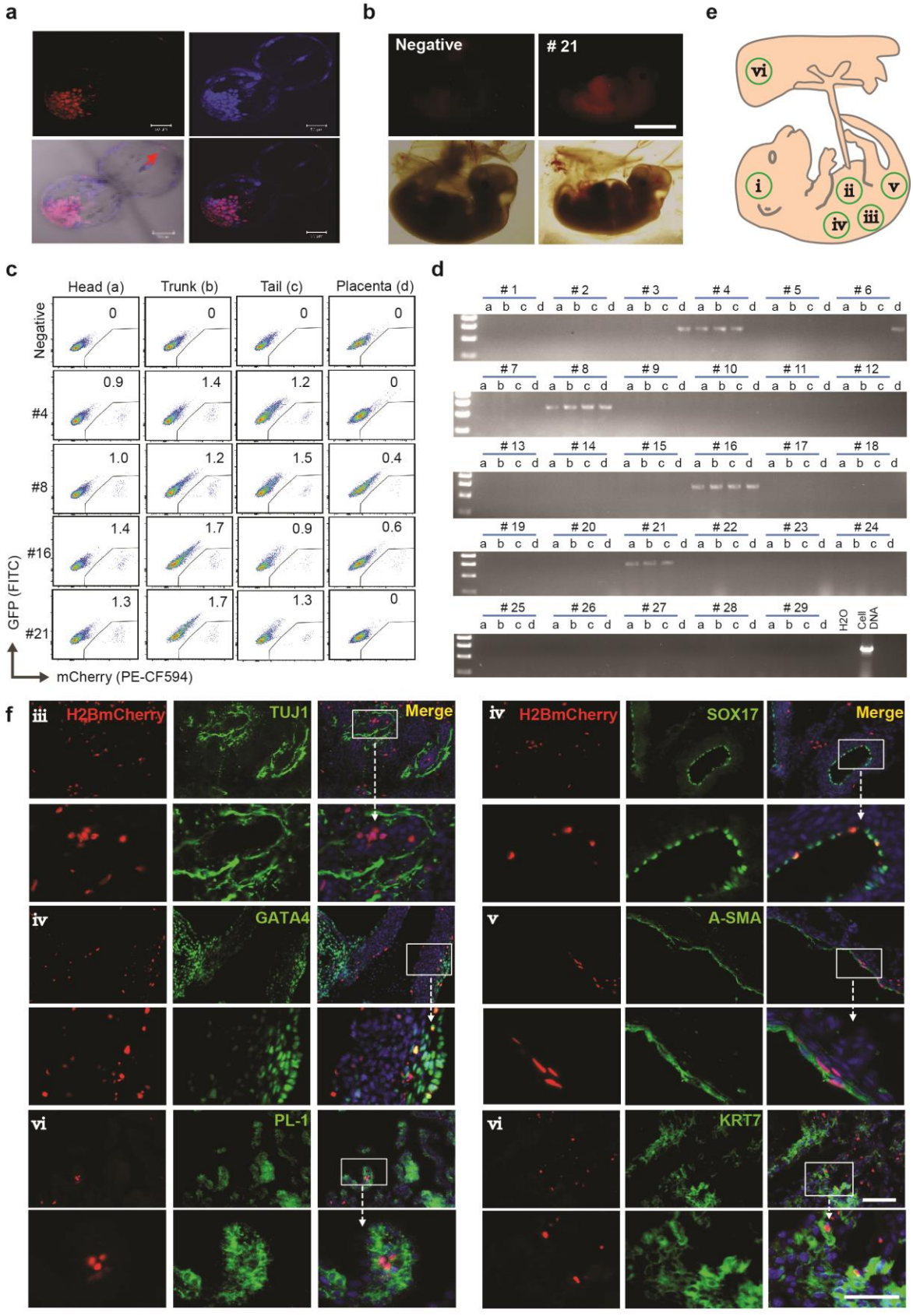
a
b
Negative
21
e
vi
i
ii
iii
iv
v
c
Head (a)
Trunk (b)
Tail (c)
Placenta (d)
Negative
#4
#8
#16
#21
0
0
0
0
0.9
1.4
1.2
0
1.0
1.2
1.5
0.4
1.4
1.7
0.9
0.6
1.3
1.7
1.3
0
GFP (FITC)
mCherry (PE-CF594)
d
1
2
3
4
5
6
7
8
9
10
11
12
13
14
15
16
17
18
19
20
21
22
23
24
25
26
27
28
29
a b c d
H2O
Cell DNA
f
iii
H2BmCherry
TUJ1
Merge
iv
GATA4
vi
PL-1
iv
H2BmCherry
SOX17
Merge
v
A-SMA
vi
KRT7

Supplementary Figure 3

***In vivo* differentiation potential of pEPSCs**

a. Participation of pEPSCs in preimplantation embryo development. H2B-mCherry-expressing donor pEPSCs^{iPS} were injected into day 5 host pig parthenogenetic embryos, which developed to blastocysts. H2BmCherry^{+} donor cells were found in both the inner cell mass and the trophectoderm (arrowed). Scale bar: 50 μm. The experiments were repeated independently three times with similar results. **b**. Whole-mount fluorescence and bright field images of 27-day pig conceptuses derived from preimplantation embryos injected with H2BmCherry^{+} pEPSCs^{Emb}, showing mCherry^{+} cells in chimera #21. Scale bar: 1.0 cm. **c**. Chimeras were processed with half of which were fixed for immunofluorescence analysis, and the other half for FACS and DNA genotyping. To prepare cells for FACS analysis, tissues of each embryo were isolated from head (a), trunk (b), tail (c), and the placenta (d), and were dissociated to single cells and selected for donor H2BmCherry^{+} cells. The dissociated cells were also used for preparing genomic DNA samples for PCR analysis. **d**. PCR genotyping for mCherry DNA using the genomic DNA samples. mCherry DNA was detected only in the embryos that were mCherry^{+} by flow cytometry analysis. **e.** Schematic diagram of day 26-28 pig chimera conceptuses. The circles mark the tissue areas where tissue sections were taken for immunostaining and imaging shown in (**f**). **f**. Immunofluorescence analysis of cryosections of day 26-28 mCherry^{+} conceptuses or chimeric embryos and placentas for H2BmCherry^{+} cells in different tissues. The antibodies used include TUJ1 for neurons (Chimera #16); SOX17 and GATA4 for endodermal derivatives (Chimera #21); a-SMA for mesodermal derivatives (Chimera #21); PL-1 and KRT7 for trophoblasts (placenta of Chimera #6). H2BmCherry, GATA4 and SOX17 were found in the nucleus, whereas TUJ, A-SMA, KRT7 and PL-1 were not nuclear localised. For **b-d** and **f**, the experiments were repeated independently three times with similar results. Scale bar: 100 μm.

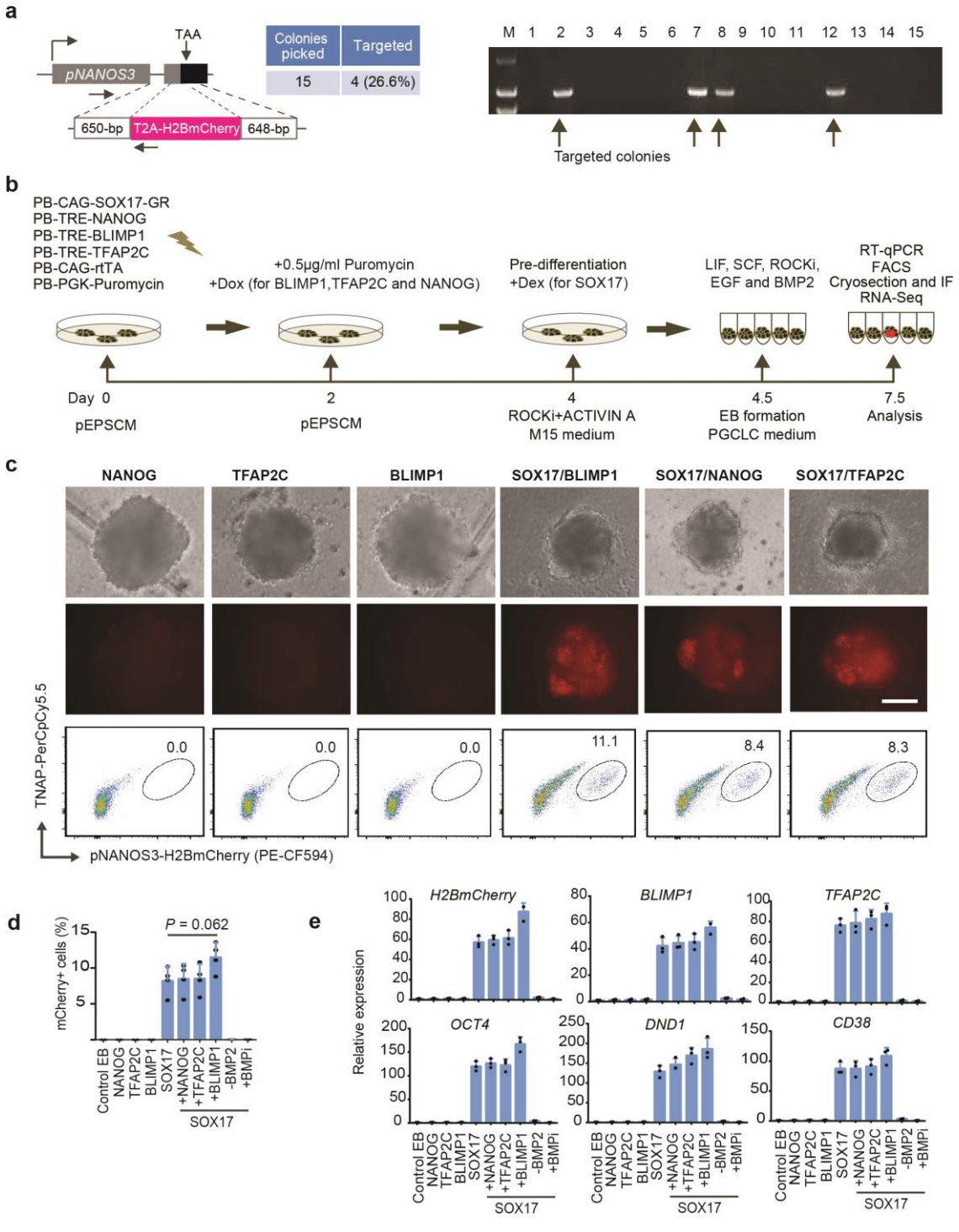
a
TAA
pNANOS3
650-bp
T2A-H2BmCherry
648-bp
Colonies picked
Targeted
15
4 (26.6%)
M 1 2 3 4 5 6 7 8 9 10 11 12 13 14 15
Targeted colonies
b
PB-CAG-SOX17-GR
PB-TRE-NANOG
PB-TRE-BLIMP1
PB-TRE-TFAP2C
PB-CAG-rtTA
PB-PGK-Puromycin
+0.5μg/ml Puromycin
+Dox (for BLIMP1,TFAP2C and NANOG)
Pre-differentiation
+Dex (for SOX17)
LIF, SCF, ROCKi,
EGF and BMP2
RT-qPCR
FACS
Cryosection and IF
RNA-Seq
Day 0
pEPSCM
2
pEPSCM
4
ROCKi+ACTIVIN A
M15 medium
4.5
EB formation
PGCLC medium
7.5
Analysis
c
NANOG
TFAP2C
BLIMP1
SOX17/BLIMP1
SOX17/NANOG
SOX17/TFAP2C
TNAP-PerCpCy5.5
pNANOS3-H2BmCherry (PE-CF594)
0.0
0.0
0.0
11.1
8.4
8.3
d
P = 0.062
mCherry+ cells (%)
Control EB
NANOG
TFAP2C
BLIMP1
SOX17
+NANOG
+TFAP2C
+BLIMP1
-BMP2
+BMPi
SOX17
e
H2BmCherry
BLIMP1
TFAP2C
OCT4
DND1
CD38
Relative expression
Control EB
NANOG
TFAP2C
BLIMP1
SOX17
+NANOG
+TFAP2C
+BLIMP1
-BMP2
+BMPi
SOX17

Supplementary Figure 4

Differentiation of pEPSCs to pPGCLCs

a. Generation of the *NANOS3-H2BmCherry* reporter EPSCs^{Emb} by targeting the *H2B-mCherry* cassette to the *NANOS3* locus. In the targeted allele, the *T2A-H2B-mCherry* sequence was in frame with the last coding exon of the pig *NANOS3* locus with the stop codon TAA being deleted. We generated gRNA plasmids targeting specifically to the region covering the *NANOS3* stop codon, and 4 out 15 colonies picked for genotyping were correctly targeted. After expansion, those targeted pEPSCs retained a normal karyotype. **b**. Diagram illustrating the strategy for expressing exogenous genes in pEPSCs^{Emb} for pPGCLC specification and differentiation (see Methods for details). **c**. Expression of *NANOG*, *BLIMP1* and *TFAP2C* individually or in combination with *SOX17* in the pPGCLCs (H2BmCherry^{+}) in EBs differentiation from *NANOS3-H2BmCherry* reporter EPSCs^{Emb}. Scale bars: 100 μm. **d.** Quantitation of NANOS3-H2BmCherry positive cells in (**c**). n = 4 independent experiments. Data are mean ± s.d. *P* values were calculated using a two-tailed t-test. **e**. RT-qPCR analysis of PGC genes. RNA samples were prepared from day 3 EBs of pEPSCs that expressed transgenes individually or in combinations following the pPGCLC induction protocol in **b**. Expression levels were normalized to *GAPDH*. n = 3 independent experiments. Data are mean ± s.d.. Statistical source data are provided in Supplementary table 10.

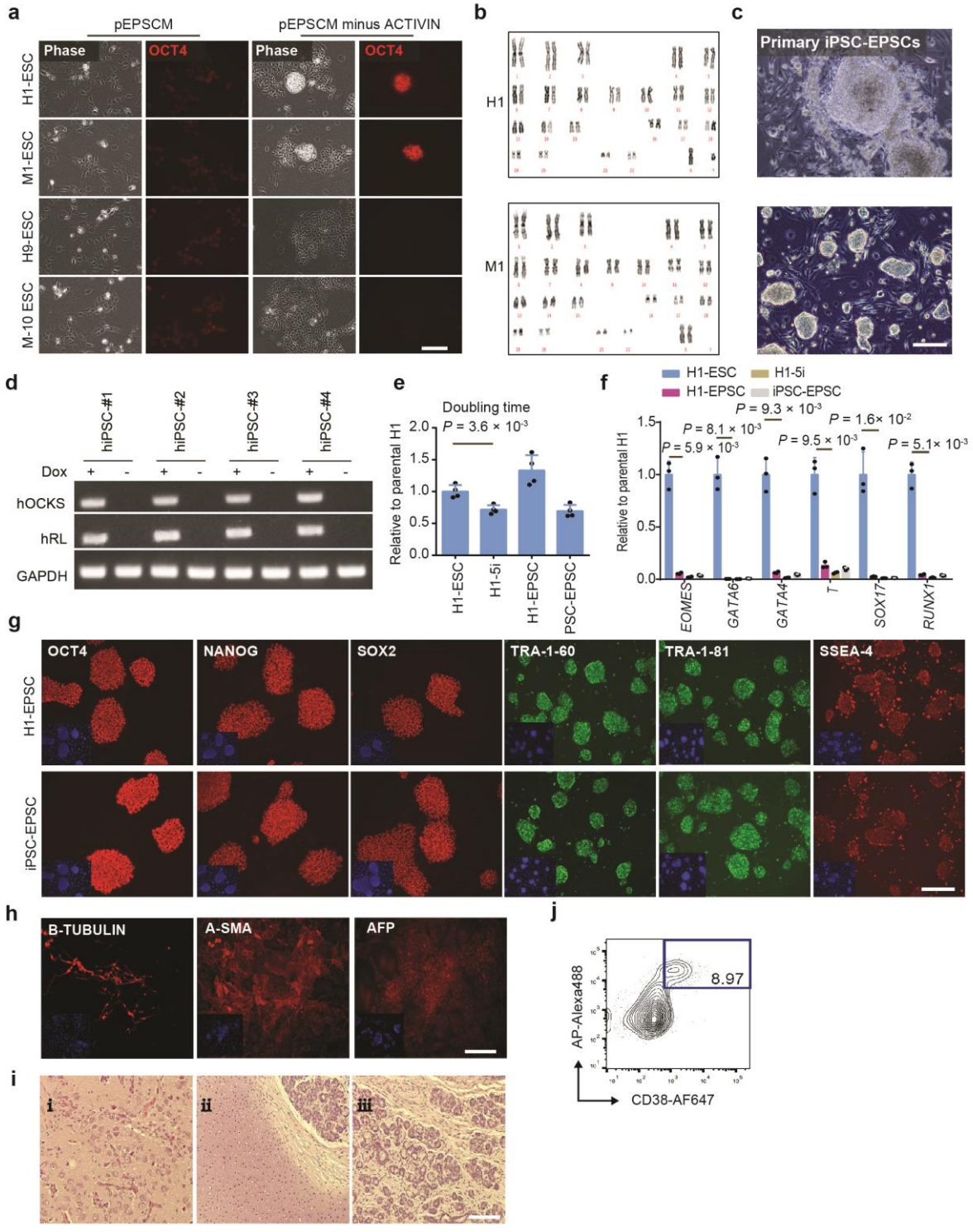
a
pEPSCM
pEPSCM minus ACTIVIN
Phase
OCT4
H1-ESC
M1-ESC
H9-ESC
M-10 ESC
b
H1
M1
c
Primary iPSC-EPSCs
d
hiPSC-#1
hiPSC-#2
hiPSC-#3
hiPSC-#4
Dox
hOCKS
hRL
GAPDH
e
Doubling time
P = 3.6 × 10-3
Relative to parental H1
H1-ESC
H1-5i
H1-EPSC
PSC-EPSC
f
H1-ESC
H1-5i
H1-EPSC
iPSC-EPSC
P = 9.3 × 10-3
P = 1.6× 10-2
P = 8.1 × 10-3
P = 5.9 × 10-3
P = 9.5 × 10-3
P = 5.1× 10-3
Relative to parental H1
EOMES
GATA6
GATA4
T
SOX17
RUNX1
g
OCT4
NANOG
SOX2
TRA-1-60
TRA-1-81
SSEA-4
H1-EPSC
iPSC-EPSC
h
B-TUBULIN
A-SMA
AFP
i
i
ii
iii
j
8.97
AP-Alexa488
CD38-AF647

Supplementary Figure 5

Establishment and characterisation of human EPSCs

a. Images of H1, H9, M1 and M10 human ESC colonies in pEPSCM or in pEPSCM without ACTIVIN A. Expression of OCT4 was detected by immunostaining. **b**. Normal karyotype in H1-EPSCs and M1-EPSCs after 25 passages in hEPSCM (10/10 metaphases scored were normal). **c**. Primary iPSC colony (top) and established cultures of iPSCs (bottom) in hEPSCM reprogrammed from human fibroblasts by Dox-inducible expression of exogenous *OCT4*, *MYC*, *KLF4*, *SOX2*, *LRH1* and *RARG*. **d**. Analysis of the expression of the exogenous reprogramming factors by RT-qPCR revealed no obvious leaky expression in four established iPSC lines. **e**. The relative population doubling time of H1-ESCs, H1-naïve ESCs (5i), H1-EPSCs and iPSC-EPSCs. n = 4 independent experiments. Data are mean ± s.d. *P* values were calculated using a two-tailed t-test. **f**. Expression of lineage markers (*EOMES*, *GATA4*, *GATA6*, *T*, *SOX17* and *RUNX1*) in H1-ESCs, H1-naïve ESCs (5i), H1-EPSCs and iPSC-EPSCs. n = 3 independent experiments. Data are mean ± s.d. *P* values were calculated between H1-ESCa and H1-EPSCs using a two-tailed t-test **g**. Immunostaining of H1-EPSCs and iPSC-EPSCs for pluripotency factors and cell surface markers. **h.** *In vitro* differentiation of H1-EPSCs to the germ layer lineages. **i.** The presence of cartilage (mesoderm. I), glandular epithelium (endoderm. II) and mature neural tissue (glia and neurons, ectoderm. III) in teratomas derived from hEPSCs. H&E staining. **j**. FACS analysis for expression of CD38 and TNAP on PGCLCs of H1-EPSCs. The induction of PGCLCs was performed on at least two human EPSC lines. Relative expression levels were normalized to *GAPDH*. For **a**, **c-d** and **g-j**, the experiments were repeated independently three times with similar results. Statistical source data are presented in Supplementary table 10. Scale bars: 100 μm.

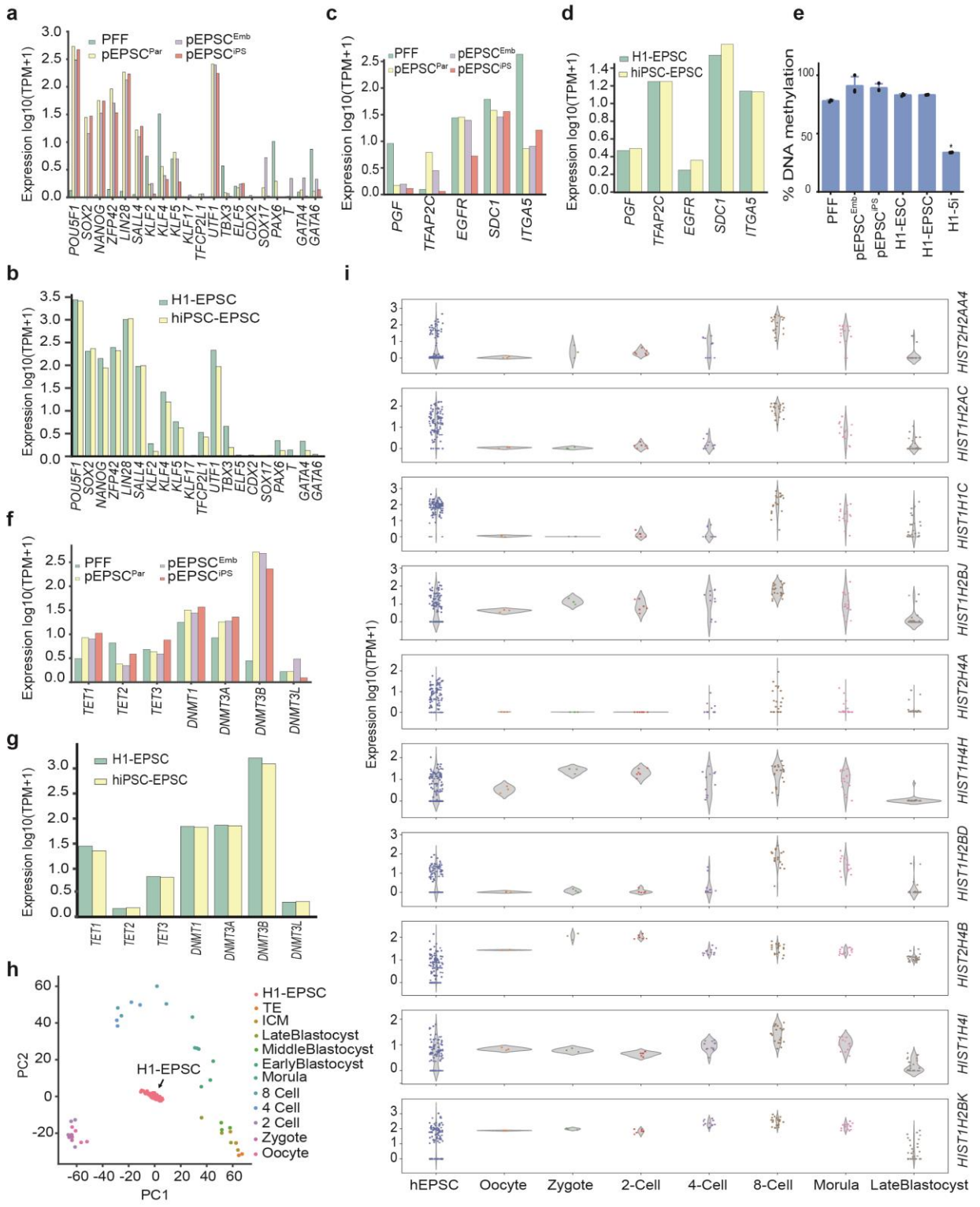
a
Expression log10(TPM+1)
PFF
pEPSC^Par
pEPSC^Emb
pEPSC^iPS
POU5F1
SOX2
NANOG
ZFP42
LIN28
SALL4
KLF2
KLF4
KLF5
KLF17
TFCP2L1
UTF1
TBX3
ELF5
CDX2
SOX17
PAX6
T
GATA4
GATA6
b
H1-EPSC
hiPSC-EPSC
c
PGF
TFAP2C
EGFR
SDC1
ITGA5
d
e
% DNA methylation
H1-ESC
H1-EPSC
H1-5i
f
TET1
TET2
TET3
DNMT1
DNMT3A
DNMT3B
DNMT3L
g
h
PC1
PC2
TE
ICM
LateBlastocyst
MiddleBlastocyst
EarlyBlastocyst
Morula
8 Cell
4 Cell
2 Cell
Zygote
Oocyte
i
HIST2H2AA4
HIST1H2AC
HIST1H1C
HIST1H2BJ
HIST2H4A
HIST1H4H
HIST1H2BD
HIST2H4B
HIST1H4I
HIST1H2BK
hEPSC
Oocyte
Zygote
2-Cell
4-Cell
8-Cell
Morula
LateBlastocyst

Supplementary Figure 6

RNAseq analysis of human and porcine EPSC transcriptome

a-b. Expression of pluripotency and lineage genes in porcine (**a**) or human (**b**) EPSCs. **c-d.** Expression of trophoblast related genes in porcine (**c**) or human (**d**) EPSCs. **e**. Global DNA methylation levels in porcine and human EPSCs. H1-5i human naïve ESCs was included in the analysis. n = 3 independent experiments. Data are mean ± s.d. $^{*}p < 0.01$, comparison of H1-5i human naïve ESCs with H1-ESCs and H1-EPSCs. The *P* values were computed by two-tailed t-test and are presented in Supplementary table 10. **f-g**. RNAseq analysis of expression of genes encoding enzymes for DNA methylation or demethylation in porcine (**f**) and human (**g**) EPSCs. **h**. PCA of scRNAseq data of human H1-EPSCs and that of human preimplantation embryos (data from ref. 38). H1-EPSCs (lower panel, n=96), Oocyte (n=4), Zygote (n=5), 2c-ell (n=4), 4-cell (n=4), 8-cell (n=4), Morula (n=4), ICM (n=3), EarlyBlastocyst (n=3), MiddleBlastocyst (n=3), LateBlastocyst (n=3), TE (n=3). i. Violin plots of the expression levels of histone genes in human EPSCs (this study) and in human preimplantation embryos at various dvelopemntal stages (ref.38). H1-EPSCs (n=96), Oocyte (n=3), zygote (n=3), 2-cell (n=6), 4-cell (n=12), 8-cell (n=20), morulae (n=16), Late blastocyst (n=30). Gene expression (TPM) was quantified by salmon and the values of log10(TPM + 1). Gene expression level in individual cells (represented by dots to show the distribution of the data) was superimposed on the violin plot.

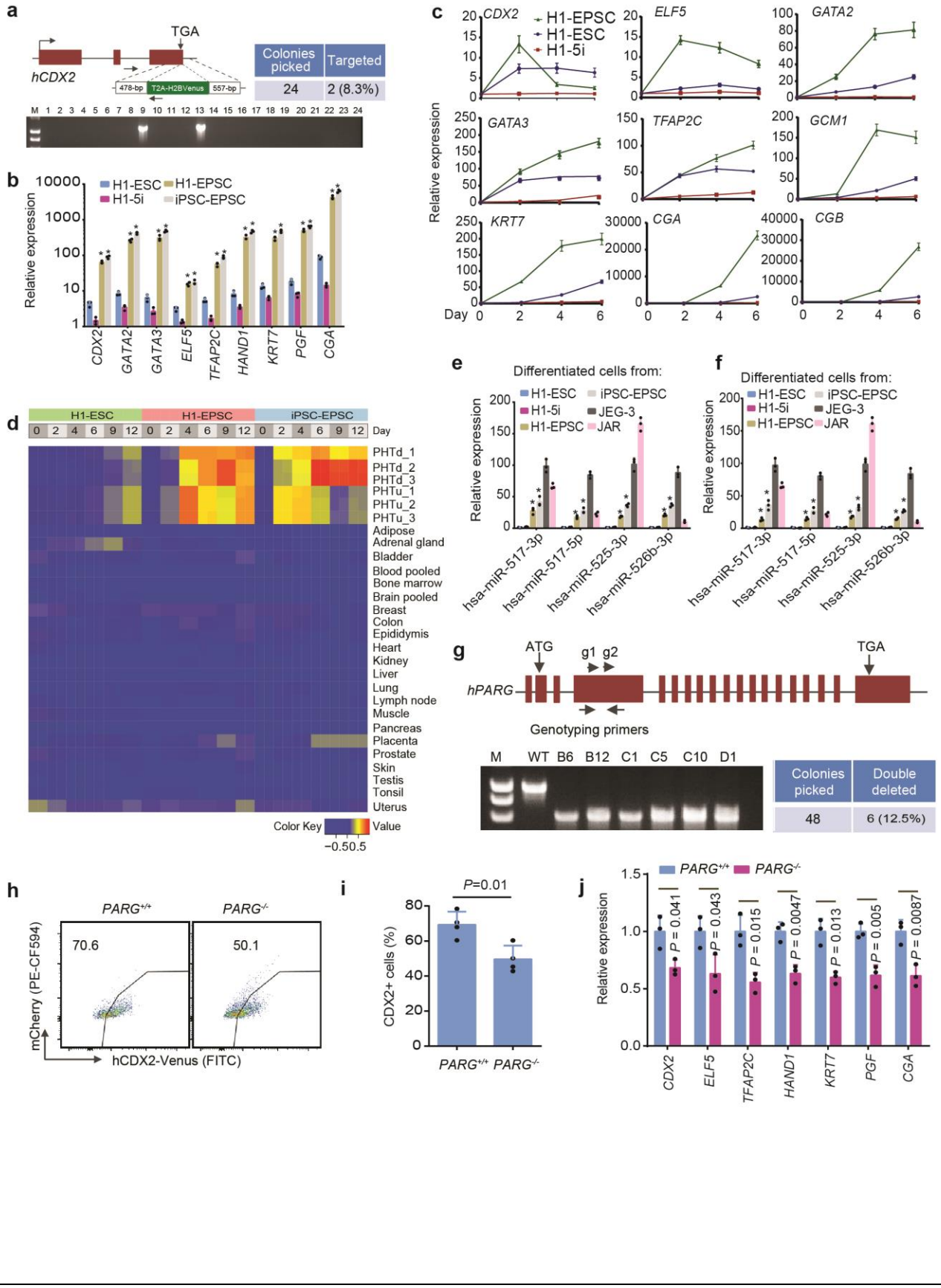
a
TGA
hCDX2
478-bp
T2A-H2BVenus
557-bp
Colonies picked
Targeted
24
2 (8.3%)
M 1 2 3 4 5 6 7 8 9 10 11 12 13 14 15 16 17 18 19 20 21 22 23 24
b
H1-ESC
H1-EPSC
H1-5i
iPSC-EPSC
Relative expression
CDX2
GATA2
GATA3
ELF5
TFAP2C
HAND1
KRT7
PGF
CGA
c
H1-EPSC
H1-ESC
H1-5i
CDX2
ELF5
GATA2
GATA3
TFAP2C
GCM1
KRT7
CGA
CGB
Relative expression
Day
d
H1-ESC
H1-EPSC
iPSC-EPSC
Day
PHTd_1
PHTd_2
PHTd_3
PHTu_1
PHTu_2
PHTu_3
Adipose
Adrenal gland
Bladder
Blood pooled
Bone marrow
Brain pooled
Breast
Colon
Epididymis
Heart
Kidney
Liver
Lung
Lymph node
Muscle
Pancreas
Placenta
Prostate
Skin
Testis
Tonsil
Uterus
Color Key
Value
e
Differentiated cells from:
H1-ESC
H1-5i
H1-EPSC
iPSC-EPSC
JEG-3
JAR
Relative expression
hsa-miR-517-3p
hsa-miR-517-5p
hsa-miR-525-3p
hsa-miR-526b-3p
f
Differentiated cells from:
g
ATG
g1 g2
TGA
hPARG
Genotyping primers
M
WT
B6
B12
C1
C5
C10
D1
Colonies picked
Double deleted
48
6 (12.5%)
h
PARG+/+
PARG-/-
70.6
50.1
mCherry (PE-CF594)
hCDX2-Venus (FITC)
i
P=0.01
CDX2+ cells (%)
PARG+/+
PARG-/-
j
PARG+/+
PARG-/-
Relative expression
P = 0.041
P = 0.043
P = 0.015
P = 0.0047
P = 0.013
P = 0.005
P = 0.0087
CDX2
ELF5
TFAP2C
HAND1
KRT7
PGF
CGA

Supplementary Figure 7

Trophoblast differentiation of hEPSCs

a. Generation of the *CDX2-H2BVenus* reporter EPSC line where the *T2A-H2BVenus* was in frame with the last coding exon of *CDX2* gene with the TGA stop codon being deleted. The reporter EPSCs were subsequently cultured in hEPSCM, the FGF-containing ESC medium or in the 5i condition for subsequent analyses. **b-c**. Expression of trophoblast-related genes analyzed by RT-qPCR of trophoblasts produced after 4-day BMP4 treatment (**b**) or by SB431542+PD173074+BMP4 sampled at several time points (**c**). Relative expression levels were normalized to *GAPDH*. *$p < 0.01$ compared with H1-ESCs and H1-5i naïve cells. n = 3 independent experiments. Data are mean ± s.d. The precise *P* values were computed by two-tailed t-test and are presented in Supplementary table 10. **d**. Pearson correlation coefficient of gene expression in cells differentiated from H1-ESCs, H1-EPSCs and iPSC-EPSCs, incorporating published data (ref. 43) of primary human undifferentiated (PHTu) and differentiated trophoblasts (PHTd), and human tissues. **e**. C19MC miRNAs in EPSCs or ESCs treated with SB431542 for six days. JEG-3 and JAR represent extravillous trophoblasts and villous trophoblast cells, respectively. **f**. Expression of the same miRNAs in the BMP4 (4-day) treated EPSCs and ESCs. *$p < 0.05$ compared with H1-ESCs. n = 3 independent experiments. Data are mean ± s.d. The precise *P* values were computed by two-tailed t-test and are provided in Supplementary table 10. miRNA expression levels are normalized to miR-103a. **g**. CRISPR/Cas9 mediated deletion of ~350bp in *PARG* exon 4 using two gRNAs (g1, g2) in *CDX2-H2BVenus* reporter hEPSCs. 6 out of 48 clones picked were bi-allelic mutants by PCR and sequencing. **h**. Trophoblast differentiation of *PARG* homozygous deletion CDX2-reporter EPSC cells ($PARG^{-/-}$) under TGFβ inhibition for four days and analysed by flow cytometry. The experiments were repeated independently four times with similar results. **i**. The percentages of $Venus^{+}$ cells as in (**h**). n = 4 independent experiments. Data are mean ± s.d. *P* values were computed by two-tailed t-test. Similar results were obtained using two independent $PARG^{-/-}$ hEPSC lines. **j**. RT-qPCR analysis of trophoblast genes in WT or $PARG^{-/-}$ H1-

EPSCs after 6 days of SB431542 treatment. n = 3 independent experiments. Data are mean ± s.d. *P* values were computed by two-tailed t-test. Expression levels are normalized to *GAPDH*. Statistical source data are presented in Supplementary table 10.

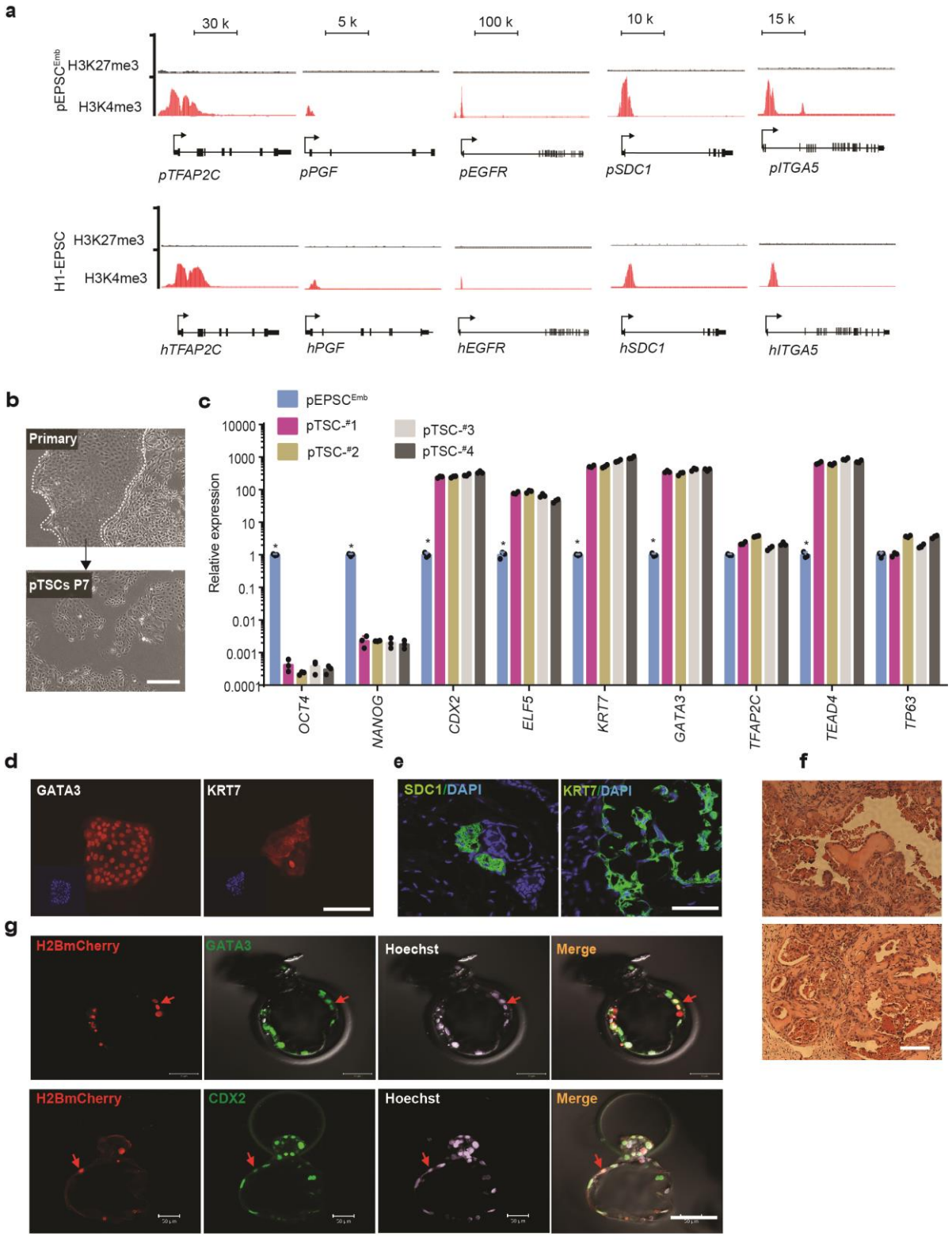
a
30 k
5 k
100 k
10 k
15 k
pEPSC^Emb
H3K27me3
H3K4me3
pTFAP2C
pPGF
pEGFR
pSDC1
pITGA5
H1-EPSC
H3K27me3
H3K4me3
hTFAP2C
hPGF
hEGFR
hSDC1
hITGA5
b
Primary
pTSCs P7
c
pEPSC^Emb
pTSC-#1
pTSC-#2
pTSC-#3
pTSC-#4
Relative expression
10000
1000
100
10
1
0.1
0.01
0.001
0.0001
OCT4
NANOG
CDX2
ELF5
KRT7
GATA3
TFAP2C
TEAD4
TP63
d
GATA3
KRT7
e
SDC1/DAPI
KRT7/DAPI
f
g
H2BmCherry
GATA3
Hoechst
Merge
H2BmCherry
CDX2
Hoechst
Merge

Supplementary Figure 8

Derivation and characterisation of trophoblast stem cell-like cells (pTSCs) from porcine EPSCs

a. H3K27me3 and H3K4me3 marks at the loci encoding factors associated with placenta development in $pEPSC^{Emb}$ and human H1-EPSCs. **b**. Images of primary TSC colonies (top) formed from individual $pEPSC^{Emb}$ on day 7 cultured in human TSC condition, and of established pTSCs at passage 7 (bottom). Dashed lines mark the area of putative trophoblasts, which were picked for establishing stable pTSC lines. **c**. RT-qPCR analysis of pluripotency and trophoblast genes in four pTSC lines and their parental $pEPSC^{Emb}$. n = 3 independent experiments. Data are mean ± s.d. $^{*}p < 0.01$ comparison between pEPSCs to pTSCs. *P* values were computed by two-tailed t-test and provided in Supplementary table 10. Expression levels are normalized to *GAPDH*. **d**. Expression of trophoblast factors GATA3 and KRT7 in pTSCs detected by immunostaining. DAPI stained nuclei. **e**. Confocal image of immunostaining of sections of lesions formed by pTSCs in NOD-SCID mice for cells expressing SDC1 and KRT7. **f**. Histology of the pTSC-derived lesions. H&E staining. **g**. Confocal images of immunostaining of porcine blastocysts 1 to 2 days following injection of H2B-mCherry-expressing pTSCs into porcine parthenogenetic or IVF morulae and early blastocysts (n = 50 blastocysts in two injections). Arrow indicates $H2B\text{-}mCherry^{+}$ cells in the trophectoderm which expressed the porcine trophectoderm transcription factor GATA3 and CDX2. For **a-b** and **d-g**, the experiments were repeated independently three times with similar results. Statistical source data are presented in Supplementary table 10. Scale bars: 100 μm.